UNCLASSIFIED

AFOSR 1666
MONITORING AGENCY DOCUMENT NO:
ASTIA DOCUMENT NO: AD

Max - Planck - Institut für Strömungsforschung
Göttingen

TECHNICAL REPORT

EXPERIMENTAL INVESTIGATIONS ON THE SCATTERING OF SOUND BY TURBULENCE

By
Dieter W. Schmidt

Göttingen
July 1961

The research reported in this document has been sponsored by the Air Force Office of Scientific Research of the AIR RESEARCH AND DEVELOPMENT COMMAND, USAF, under Contract AF 61 (514)-1143, through its European office, ARDC.

Max-Planck-Institut für Strömungsforschung
Göttingen

TECHNICAL REPORT

EXPERIMENTAL INVESTIGATIONS ON THE SCATTERING OF SOUND BY TURBULENCE

By

Dieter W. Schmidt

Göttingen
July 1961

The research reported in this document has been sponsored by the AIR RESEARCH AND DEVELOPMENT COMMAND, USAF, under Contract AF 61(514)-1143, through the European Office, ARDC.

TABLE OF CONTENTS

SUMMARY

Experimental investigations of the scattering of sound by turbulence were performed in a wind tunnel. The turbulence was produced by grids of parallel circular rods (with diameters of 0.1 to 1.0 cm and grid meshlengths of 0.5 to 2.5 cm); the sound frequencies covered a range of 100 to 500 kcps. Main flow velocities between 13 and 70 $m \cdot s^{-1}$ were employed in the test duct. The length of the measuring sound path in the turbulent flow was 30 cm; it was perpendicular to the rods of the grid and parallel to the grid plane, the distances between the grid plane and the sound path ranging from 5 to 21 cm. Disturbances of the measurements due to reflections of sound waves at the tunnel walls were avoided by the application of short sound pulses.

The dependence of the damping of the sound waves on the sound frequency, the Mach number of the turbulence, the length of the sound path in the turbulent flow and a predominant direction of the turbulent eddies was measured. The theoretical predictions given in [1 to 5] were well confirmed and partly extended. In the range of the parameters which is of interest for practical use the most important results are the proportionality of the damping to the square of the sound frequency and to the square of the turbulent Mach number.

Based on the measurements and the theoretical considerations, a formula is derived which is applicable to the damping of sound by turbulent scattering in the atmosphere. This scattering process is of interest for the damping of aircraft noise.

1. Introduction.

The present experimental investigation deals with a problem of the interaction of sound and turbulence, namely the scattering of sound by turbulence. During the last years the turbulent scattering of sound has found a great technical interest. It has, for instance, considerable influence upon the damping of sound waves in the free atmosphere. Especially with regard to the use of jet-planes in air traffic, a detailed knowledge of this damping effect is desired for planning airfields and arranging the courses of airplanes suitably, so that people are not troubled excessively by the very intensive noise which is radiated from such airplanes. Further, within the turbulent jet itself, where this noise is generated, the scattering of sound by turbulence may be assumed to have a great influence on the propagation of the sound waves, thus affecting the polar distribution and the intensity of the radiated sound considerably. In addition, the scattering of sound is important for the audibility and intelligibility of acoustical signals in the free atmosphere and in the sea as well as for the damping of sound which is propagated through pipes containing a turbulent flow.

As a basis for a successful treatment of these problems a complete understanding of the physical effect of the scattering of sound by turbulence is needed. The investigations, which were performed at the Max-Planck-Institut für Strömungsforschung in Göttingen, shall be a contribution to the basic research concerning this effect. The theoretical investigation, which has been performed by E.-A.Müller and K.R.Matschat, was finished in 1959 by a Technical Report entitled "The scattering of sound by a single vortex and by turbulence" [1]. It yielded comprehensive quantitative results about the changes of a plane sound field which are caused by turbulent scattering. The present experimental investigations confirm and extend the theoretical results.

List of Symbols

a_o	velocity of sound in air $[cm \cdot s^{-1}]$
B	width of the test section in the wind tunnel [cm]
d	distance of the turbulence grid from the sound beam axis (measured along a streamline of the mean flow) [cm]
d_z	distance behind the turbulence grid at which the widths of the single wakes behind the rods become equal to the meshlength M [cm]
D	diameter of the rods of the turbulence grid [cm]
H	height of the test section in the wind tunnel [cm]
I^{lam}	sound intensity in the case of laminar flow [arbitrary unit]
I^{turb}	same as I^{lam}, but in the case of turbulent flow
I^{lam}_{meas}	measured value of sound intensity in the case of laminar flow [arbitrary unit]
I^{turb}_{meas}	same as I^{lam}_{meas}, but in the case of turbulent flow
k_1	dimensionless factor in eq.(30) and (31)
k_2	dimensionless factor in eq.(31)

$$L_n = \int_0^\infty \frac{\overline{u_x(y_1) \cdot u_x(y_1+y)}}{\sqrt{\overline{u_x(y_1)^2}} \cdot \sqrt{\overline{u_x(y_1+y)^2}}} \, dy$$ lateral macroscale of the turbulence [cm or m]

$$L_p = \int_0^\infty \frac{\overline{u_x(x_1) \cdot u_x(x_1+x)}}{\sqrt{\overline{u_x(x_1)^2}} \cdot \sqrt{\overline{u_x(x_1+x)^2}}} \, dx$$ longitudinal macroscale of the turbulence [cm or m]

log	Briggsian logarithm
M	meshlength of the turbulence grid (distance between the rods of the grid) [cm]
$\bar{M}$	mean Mach number of the turbulent vortices
n	number of rods in the turbulence grid
n_1, n_2	shedding frequencies of v.Kármán vortices [cps]

n_{M_1}, n_{M_2}	measured predominant frequencies in a turbulent wake [cps]
q	dynamic pressure of the mean flow [mm water]
r_a	radius of the scattering vortices [cm]
$R_a = \frac{r_a}{a_o} \cdot \nu$	dimensionless radius of the scattering vortices
s	length of the sound path in turbulent flow [cm]
$S = \frac{n_1 \cdot D}{U}$	Strouhal number
t_1	duration of the transmitted sound pulses [ms]
t_2	duration of the selected and measured part of the received sound pulses [ms]
T	time elapsing from one transmitted sound pulse to the next one [ms]
$u' = \sqrt{\overline{u_x^2} + \overline{u_y^2} + \overline{u_z^2}}$	rms value of the turbulent fluctuation velocity $[m \cdot s^{-1}]$
u_x, u_y, u_z	fluctuation velocities in x,y,z-direction, respectively $[m \cdot s^{-1}]$
$u_y' = \sqrt{\overline{u_y^2}}$	rms value of the turbulent fluctuation velocity in y-direction $[m \cdot s^{-1}]$
U	velocity of mean flow (prallel to x-direction) $[m \cdot s^{-1}]$
x, y, z	Cartesian space coordinates, x alined with mean flow
ΔI	damping of sound due to turbulent scattering [db]
θ	angle between the axis of a scattering vortex and the propagation direction of the incident sound waves
θ'	angle between the rods of the turbulence grid and the propagation direction of the incident sound waves
ν	frequency of sound [cps or kcps]
τ_1	delay of received sound pulses against the transmitted pulses [ms]
τ_2	delay of the leading edge of the selector pulses against the leading edge of the received sound pulses [ms]

2. Theoretical results and predictions; the problems to be investigated experimentally.

The theoretical basis for the present experimental investigation was the theory developed by E.-A.Müller and K.R.Matschat [1] for the scattering of sound by turbulence. This theory consists of two parts. In the first one the problem of the scattering of plane sound waves by a single vortex is solved. In the second one it is assumed that a field of turbulence may be described by a statistical superposition of vortices, an assumption which leads to the solution of the scattering problem for turbulence, too, the turbulence being isotropic or even extremely non-isotropic. In all cases in which calculations by other authors [2,3,4,5] exist the results obtained by them agree well with those described in [1].

The theory developed in [1] gives explicit results as well for the attenuation of sound waves by scattering as for the angular distribution of the scattered sound. The subject of the present investigation was to check and to extend the theoretical formulas, especially those for the attenuation, which are most important for the scattering in the free atmosphere.

The scattering by turbulence is governed by the following parameters of the flow field and the sound field:

1) The Mach number of turbulence $\frac{u'}{a_o} = \frac{\sqrt{\overline{u_x^2} + \overline{u_y^2} + \overline{u_z^2}}}{a_o}$ (represented in the theory [1] by the mean Mach number $\overline{M}$ of the turbulent motion),

2) the properties of the turbulence with respect to homogeneity and isotropy,

3) a characteristic length of the turbulence, represented, for instance, by a diameter L_n of the turbulent eddies (macroscale) (represented in the theory [1] by the mean radius r_a of the scattering vortices),

4) the frequency ν of the incident sound waves,

5) the length s of the sound path in the turbulent medium.

For the attenuation ΔI of the sound by turbulent scattering two asymptotic laws were established in [1] for the limiting cases $R_a = \frac{r_a}{a_o} \cdot \nu \ll 1$ and $\gg 1$, respectively, which means large wave length or small wave length of the incident sound waves as compared to the radius of the vortices. The following formulas are obtained with the assumption that the turbulence is homogeneous and that all scattering vortices have the same radius r_a and the same mean Mach number $\overline{M}$.[1] They are valid for values of $\overline{M} \cdot \frac{r_a}{a_o} \cdot \nu \ll 1$. Then, for isotropy, the damping ΔI reads

$$\Delta I = \frac{80}{63} \pi^6 \cdot \log e \cdot \overline{M}^2 \frac{s}{r_a} R_a^5 \qquad \text{for } R_a \ll 1 \qquad (1)$$

$$\Delta I = 20 \pi^3 \left(1 - \frac{2}{\pi}\right) \cdot \log e \cdot \overline{M}^2 \frac{s}{r_a} R_a^2 \qquad (2)$$
$$\text{for } R_a \gg 1 \, ,$$

and for extremely non-isotropic turbulence:

$$\Delta I = \frac{5}{2} \pi^6 \cdot \log e \cdot \sin^4 \theta (\sin^4 \theta + 4\cos^4 \theta) \, \overline{M}^2 \frac{s}{r_a} R_a^5 \qquad (3)$$
$$\text{for } R_a \ll 1$$

$$\Delta I = 80 \pi^2 \left(1 - \frac{2}{\pi}\right) \cdot \log e \cdot \sin \theta \cdot \overline{M}^2 \frac{s}{r_a} R_a^2 \qquad (4)$$
$$\text{for } R_a \gg 1 \, .$$

Here, the extremely non-isotropic turbulence is represented in an idealized kind by vortices which have parallel axes but are statistically independent from one another; θ is the angle between the direction of the axes and the normal of wave propagation of the incident sound waves.

Both for isotropic and extremely non-isotropic turbulence the law for the limiting case $R_a \ll 1$ differs from that one

---

1) With respect to the treatment of more complicated distributions of vortex radii and Mach numbers see [1]. For the present purposes they are not necessary.

for the other limiting case $R_a \gg 1$ with respect to the dependence of the damping ΔI on the frequency ν of the sound waves and the radius r_a of the vortices: In the first limiting case ΔI is proportional to ν^5 and r_a^4, in the second one proportional to ν^2 and r_a. The dependence of the damping ΔI on the mean Mach number $\overline{M}$ of the scattering vortices and the length s of the way the sound travels through the turbulent region is the same in both cases: ΔI is proportional to $\overline{M}^2$ and to s.

The transition between both asymptotic laws occurs in the vicinity of $R_a = 1$. The trace of the curve ΔI in the transition region was calculated numerically. Fig.1 shows the whole function $\Delta I = f(R_a)$ for isotropic turbulence and extremely non-isotropic turbulence with $\theta = 90^\circ$ and $\theta = 15^\circ$. With the help of the intersection points of the asymptotes, it is easy in each of these cases to obtain informations about the values r_a and $\overline{M}$ which are characteristic for the turbulence. From the two equations (1) and (2) for the asymptotes at isotropic turbulence, for instance, one gets the following formulas, in which the suffix c means the values belonging to the intersection point:

$$(\Delta I)_c = \frac{80}{63}\pi^6 \cdot \log e \cdot \overline{M}^2 \frac{s r_a^4}{a_o^5} \nu_c^5 \qquad (R_a \ll 1) \quad (5)$$

$$(\Delta I)_c = 20\,\pi^3 \left(1 - \frac{2}{\pi}\right) \cdot \log e \cdot \overline{M}^2 \frac{s r_a}{a_o^2} \nu_c^2 \qquad (R_a \gg 1)\,. \quad (6)$$

From these equations it follows

$$r_a = \frac{0.569\, a_o}{\nu_c} \qquad (7)$$

$$\overline{M}^2 = 17.9 \cdot 10^{-3} \frac{a_o}{s} \cdot \frac{(\Delta I)_c}{\nu_c} \quad . \qquad (8)$$

In the same way one obtains for non-isotropic turbulence with $\theta = 90^\circ$:

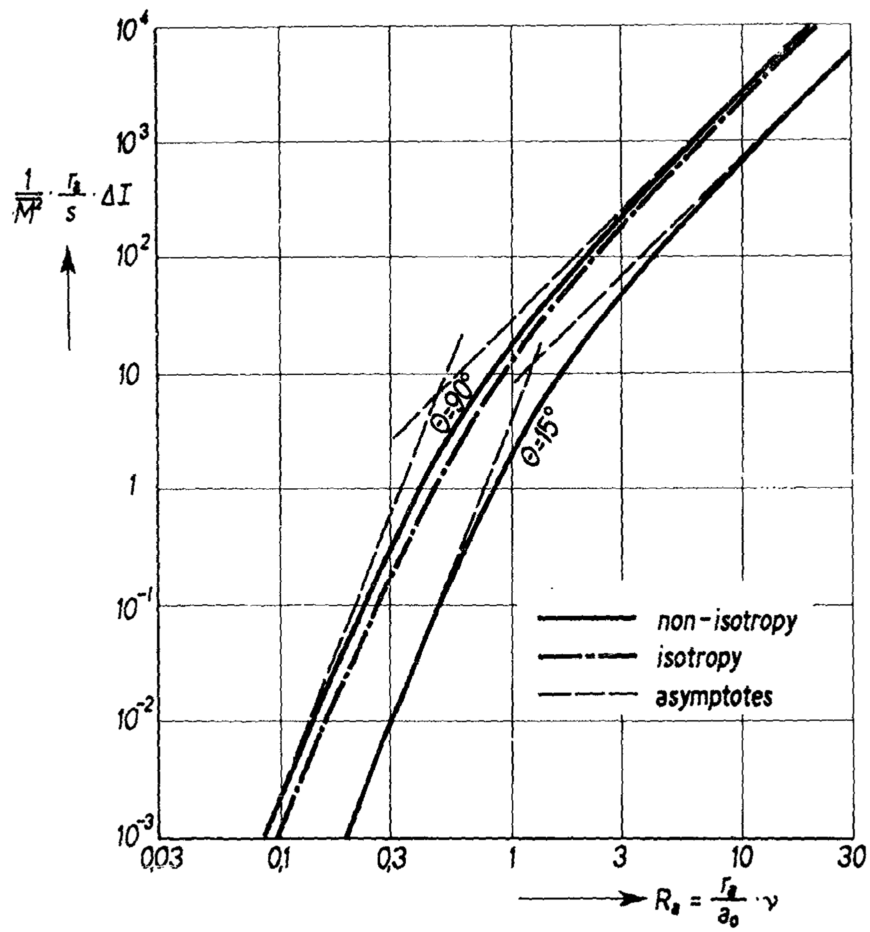

Fig.1: Theoretically derived damping of sound due to scattering by turbulence vs. the dimensionless radius of the scattering vortices (after [1]).

$$(\Delta I)_c = \frac{5}{2}\pi^6 \cdot \log e \cdot \overline{M}^2 \frac{sr_a^4}{a_o^5} \nu_c^5 \qquad (R_a \ll 1) \quad (9)$$

$$(\Delta I)_c = 80\,\pi^2 \left(1 - \frac{2}{\pi}\right) \cdot \log e \cdot \overline{M}^2 \frac{sr_a}{a_o^2} \nu_c^2 \qquad (R_a \gg 1), \quad (10)$$

and, hence,

$$r_a = \frac{0.492\ a_o}{\nu_c} \tag{11}$$

$$\overline{M}^2 = 16.3\cdot 10^{-3}\ \frac{a_o}{s}\cdot\frac{(\Delta I)_c}{\nu_c} \quad . \tag{12}$$

For this method of r_a- and $\overline{M}$-determination one would need the asymptote of the ν^5-region as well as the asymptote of the ν^2-region. It is, however, sufficient for the experimental determination of the values $(\Delta I)_c$ and ν_c belonging to the intersection point to know the damping ΔI as a function of ν within the region of $\nu \geq \nu_c$ so far as it is required for the determination of the ν^2-asymptote. As it follows from the curves of the damping in fig.1, the following relations are valid at $\nu = \nu_c$:

$$\frac{\Delta I}{(\Delta I)_c} = 0.30 \quad \text{for isotropy} \tag{13}$$

and

$$\frac{\Delta I}{(\Delta I)_c} = 0.28 \quad \text{for non-isotropy with } \Theta = 90^\circ \quad . \tag{14}$$

Another way for the determination of r_a and $\overline{M}^2$ follows, if one only knows the curve $\Delta I = f(R_a)$ in a range $\nu \geq \nu_g > \nu_c$, in which the ν^2-asymptote can be drawn and in which the deviation of the curve from the asymptote can be determined. The numerical calculations namely, which were the basis for fig.1, give a factor for each value of ν, by which the value ΔI belonging to the ΔI-curve is smaller than the value $(\Delta I)_{as}$ belonging to the ν^2-asymptote. For $R_a = 1$, for instance, one gets:

$$\left(\frac{\Delta I}{(\Delta I)_{as}}\right)_{R_a=1} = 0.58 \quad \text{for isotropy} \tag{15}$$

and

$$\left(\frac{\Delta I}{(\Delta I)_{as}}\right)_{R_a=1} = 0.60 \quad \text{for non-isotropy with } \Theta = 90^\circ \quad . \tag{16}$$

Hence, if one determines the value ν_g for which the relation (15) or (16), respectively, holds, ν_g is equal to the frequency $\nu_{R_a=1}$ belonging to $R_a = 1$. For non-isotropy, for instance, it follows:

$$r_a = \frac{a_0}{\nu_{R_a=1}} \tag{17}$$

$$\overline{M}^2 = 8.03\cdot 10^{-3}\,\frac{a_0}{s}\cdot\frac{(\Delta I)_{R_a=1}}{\nu_{R_a=1}} \quad . \tag{18}$$

Based upon these theoretical results concerning the damping of sound by turbulent scattering, the following problems can be listed for experimental research on this topic: The damping ΔI is to be investigated in dependence on

a) the frequency of sound,
b) the degree of turbulence,
c) the mean diameter of the turbulent eddies,
d) the distance which is travelled through by the sound waves,
e) the degree of non-isotropy of the turbulence,
f) (in the case of non-isotropy:) the main direction of the scattering vortices.

In the following sections experiments are reported which contribute to the solution of these problems.

3. Description of the method of measurement and of the apparatus.

3.1. Production of the turbulent air flow by a grid in a windtunnel. Arrangement of the test section. Method of measurement.

Until now most experimental investigations concerning the scattering of sound by turbulence were performed in the free atmosphere (see, for instance, [6,7,8]) or in the open sea ([9], for instance). Using this method of measurement, a great part of the test conditions, of course,

cannot be controlled, and some parameters, which are important for the scattering, cannot be determined accurately. Therefore, it was desired to perform measurements under reproducable conditions in the laboratory. With not too great expense, however, in the laboratory only turbulence can be produced, which contains vortices with diameters in the order of magnitude of centimeters (in contrary to diameters of vortices in the order of magnitude of meters or more in the free atmosphere and in the sea, respectively). From this reason, the wave length of the sound which is used for the measurements must be reduced correspondingly. This leads to the use of ultrasonics.

A block diagram of the apparatus which was used is shown in fig.2. The measurements were performed within the entrance region of a test duct, which has two favourable properties for the purpose desired: The velocity of the air flow is nearly constant over the whole cross-section of the duct, and the turbulence of the air which is sucked in from the resting air outside in the room is very weak. The flow was made turbulent by an interchangeable grid which consisted of circular rods parallel to one another. At the distance d behind the grid one gets a turbulent flow, the mean value properties of which are constant in time. At this distance the ultrasonic waves, which are propagated as a "sound beam", travel through the flow, as can be seen from the figure: The sound waves are transmitted from a sound transmitter which is placed in the bottom tunnel wall, and are received by a microphone which is placed in the tunnel wall opposite to the transmitter. Corresponding to the deflection of the sound beam due to the main flow in the duct, the receiving microphone is shifted in the downstream direction against the transmitter.[1)]

1) The shift of the microphone which is needed in order to compensate for this sound beam deflection can be calculated easily: It is the product of the height H of the test section and the Mach number U/a_0 of the main flow. Experimentally, it is found by adjusting the receiving microphone so that maximum sound intensity is received (adjustment to the axis of the sound beam).

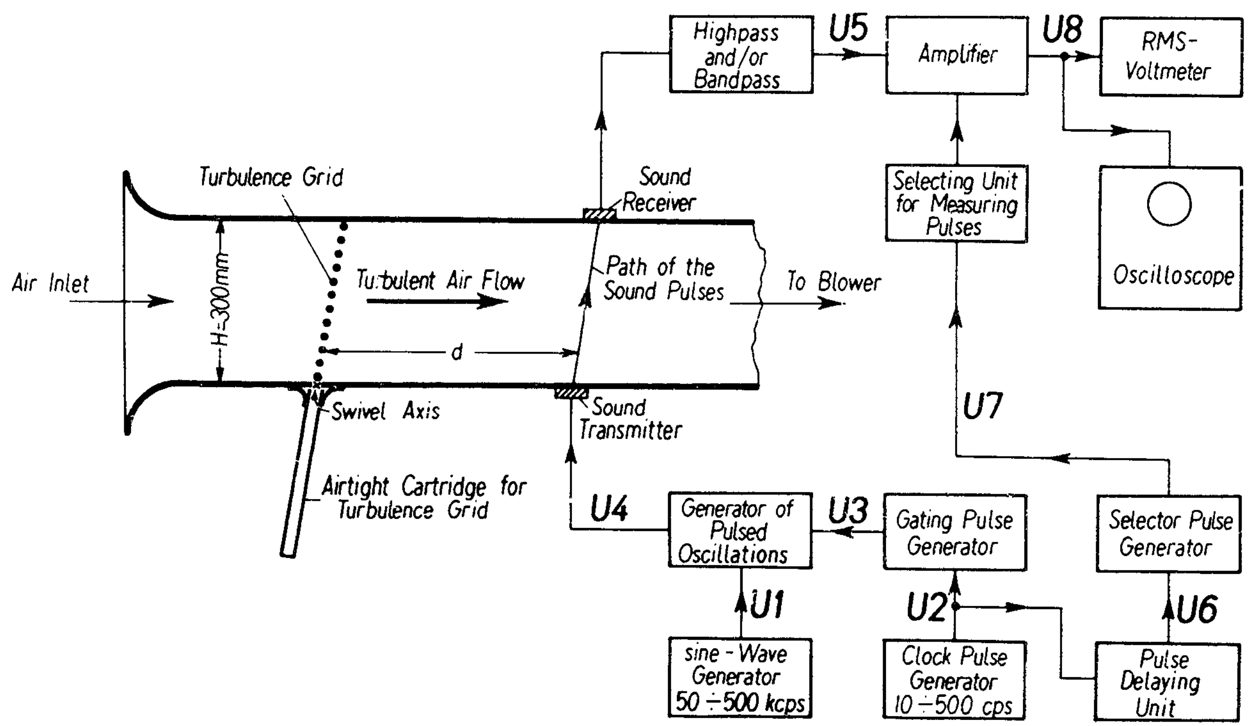

Fig.2: Block diagram of the test setup.

The turbulence producing grid was turned around the swivel axis (see fig.2) so far that it was parallel to the axis of the sound beam. In this case, notwithstanding the decay of the turbulence behind a grid, the mean turbulent properties of the flow are constant along the sound path (as well in time as in space). All parameters of the turbulence, which have been stated in Section 2. to be important for the scattering of sound, could be varied independently from one another over a broad range by varying the sizes M and D (meshlength and diameter of the rods) of the grid, the distance d of the grid from the sound beam (the position of the grid could be varied) and the velocity U of the main flow.

If one uses the test setup shown in fig.2 and if the sound is radiated continuously, inevitable superpositions of sound transmitted directly and sound reflected at the tunnel walls would be obtained. In order to avoid such disturbing superpositions, ultrasonic pulses, suitably chosen in length and recurrence frequency, were used for measurement. All reflected sound pulses need a longer time for the transmission between the sound transmitter and the receiving microphone than the pulses which are transmitted directly; hence, if the pulses are short enough, both parts can be separated from one another.

Most of the measurements reported here were performed in a windtunnel with rectangular cross-section, the height of which was H = 30 cm and the width was B = 12 cm. In this windtunnel the first of all reflected sound pulses are those, which are reflected once at the side walls of the duct. These pulses, however, are very small, their energy originating in the small side lobes of the directive pattern of the focussing sound transmitter. If, in addition, the solid side walls of the tunnel were coated with sound absorbing material (sheets of Sillan) within the region 10 cm before to 10 cm behind the sound transmitter (in flow direction), the reflections of sound at the side walls of the test duct could be reduced to an amount which did not disturb the measurements.

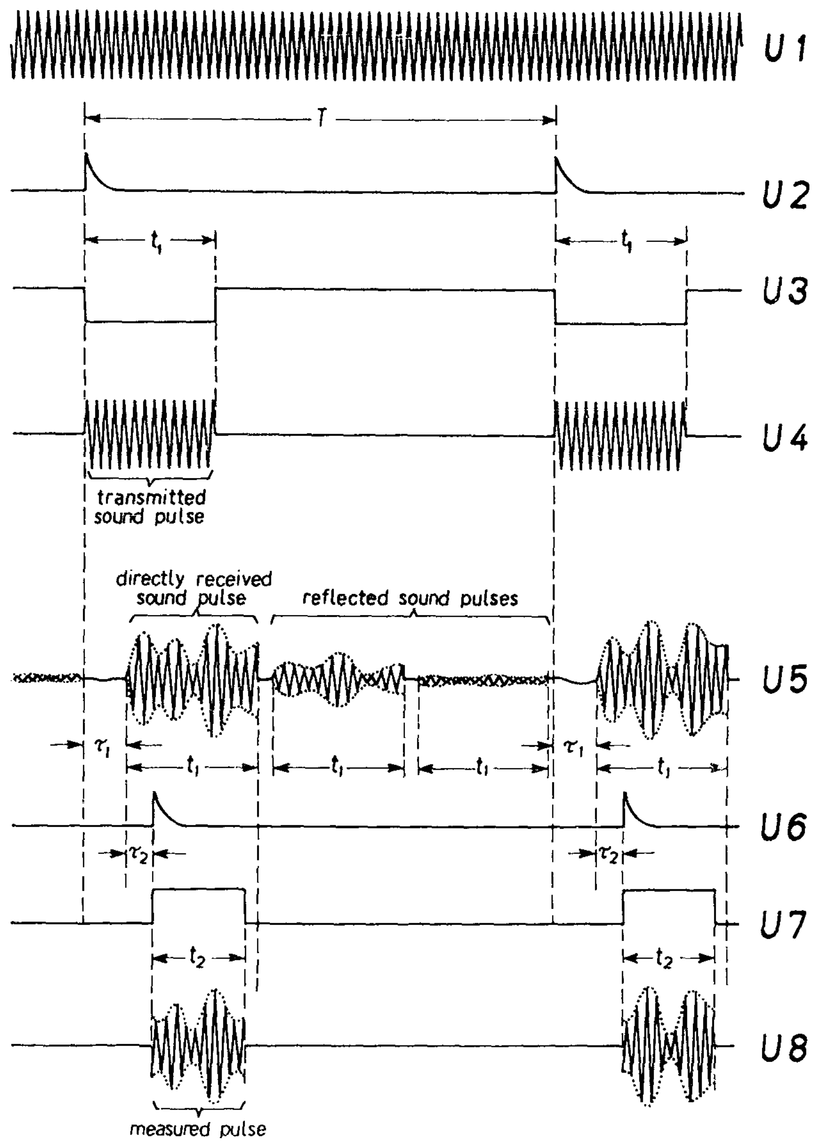

Fig.3: Schematic patterns of voltages denoted in fig.2, showing their relationships in time.

The reflections at the side walls of the wind tunnel thus being suppressed, only pulses which reach the microphone after multiple reflections at the upper and the lower wall could cause disturbances during the measurements. Of course, the distance d between the turbulence grid and the axis of the sound beam may not be too small ($d \gtrsim 10$ cm - otherwise see the paragraph after next). That one of these pulses which is received at first has an additional transmission time of 1.74 ms against the directly received pulse (according to one reflection at the upper and at the lower wall, respectively). If the duration t of the sound pulse is taken equal to 1.74 ms or smaller and if, moreover, the time T elapsing from one pulse to the following one is longer than the time in which all reflected pulses decay totally, the measuring pulses are obtained without any disturbing superposition of reflected pulses (see the voltage pattern U 5 in fig.3).

At the lowest sound frequency of 100 kcps which was used for the measurements each pulse of 1.74 ms duration contains 174 periods of sound oscillation. This number, by applying the selection described in Section 3.3., is reduced to about 120, but this number still is sufficient to permit the measurements to be evaluated in the same manner as if continuous sound waves were used.

If, however, d is reduced to values smaller than 10 centimeters (that means the turbulence grid is placed very close to the sound beam, as it is necessary to obtain highest intensities of turbulence or smallest diameters of the vortices (see Section 4.1.)), disturbances occur due to reflections at the grid. Superpositions of the measuring pulses with such reflected sound waves could, of course, be avoided by the use of much shorter sound pulses. According to a difference in the lengths of the sound paths of only some centimeters one would get pulse durations of about $t = 0.01$ ms . Such pulses, at a measuring frequency of 100 kcps, would contain only one period of oscillation, and, therefore, this possibility does not come into question. Hence, another method to avoid disturbances of

the measurements in the case $d \lesssim 10$ cm was needed, in which longer pulses could be used.

For this purpose, the phase of the reflected sound waves which were received by the receiving microphone was wobbled by values of $\pm 180^{\circ}$. A simple way for doing this was suggested by the manner in which the turbulence grid was fixed in the rectangular test duct. As can be seen from fig.2, the grid could be put into the duct (or removed out of it, respectively) out of an airtight cartridge at the bottom of the duct. By turning the grid (together with the cartridge) around the swivel axis drawn in it was inclined in the downstream direction as was mentioned on page 15 . For the intended wobbulation the inclination was altered periodically by a certain angle by means of an eccentric drive. If this angle was properly adjusted to the applied sound frequency, the desired phase wobbling ($\pm 180^{\circ}$) of the sound which is reflected at the grid was obtained, and, therefore, in the time average, it did not affect the amplitude of the measuring pulses. If the amplitude correction which is introduced by this method is relatively small, as it was true for the measurements reported here, the rms-value of the pulses can also be assumed to be well corrected in this way. In the most unfavourable case of the performed measurements, the distance d between the turbulence grid and the axis of the sound beam was 5 cm, and, at a sound frequency of 100 kcps, the proper amplitude of wobbulation has a value of ± 0.5 cm, measured at the upper end of the grid (the lower end being fixed in the swivel axis). For the evaluation of the measurements it was assumed that the grid can be regarded as being fixed in the distance $d = 5$ cm from the sound beam.

Differing from the test setup described above a test duct of circular cross section, 30 cm in diameter, was used for measuring the scattering of sound in dependence on the main direction θ' of the vortices. In this case the partial coating of the tunnel walls with sound absorbing material was unnecessary because of the much greater distance between the

"side walls" (which corresponds to a tunnel width of $B = 30$ cm in the case of rectangular cross section). In this arrangement, the turbulence grid was put into the test duct through the inlet nozzle.

The purpose of the measurements in most of the cases was to determine the damping of the sound waves by scattering due to the turbulence which is present between the sound transmitter and the receiving microphone. This damping is defined by the following equation:

$$\Delta I = 10 \log \frac{I^{lam}}{I^{turb}} \quad ; \qquad (19)$$

in this equation (the mean radiated sound intensity being constant in time) I^{lam} means the intensity of the sound which is received by the microphone in the case of laminar flow (that is, without scattering), and I^{turb} means the corresponding value if the flow is made turbulent and scattering takes place. Measurements of ΔI were made, therefore, in the following manner: At first, the turbulence grid was removed out of the test duct and the sound intensity I^{lam}_{meas} was measured in an arbitrary unit. After this the turbulence grid was inserted in the flow and, all other conditions being the same as before, an intensity I^{turb}_{meas} was measured using the same unit as for I^{lam}_{meas}. Disturbances caused by noise could be determined by extra measurements, during which no measuring sound pulses were transmitted, as well in the laminar as in the turbulent flow.[1] These disturbances are not correlated with the scattering turbulence.

[1] The noise which was produced by the blower was highly damped before reaching the test section, the connecting duct between the blower and the test section including a part 2.5 m long the walls of which were coated by sound absorbing material (sheets of Sillan). Additionally, this part of the duct was bent by an angle of 30^{o} 1.25 meters apart from its beginning.

The intensities of these noise disturbances, which were measured in the same units as I^{lam}_{meas} and I^{turb}_{meas}, were simply subtracted from the measured values I^{lam}_{meas} and I^{turb}_{meas}. Thus, one obtained the values I^{lam} and I^{turb}, from which the damping ΔI could be calculated by formula (19). The value of ΔI obtained in this way is true even if the flow without turbulence grid is not exactly laminar, because only the damping caused by the grid-produced turbulence is measured; a small amount of "zero-turbulence" has no effect on the measurement of ΔI, because it reduces the sound intensity by nearly the same factor in the "laminar" and the turbulent state of flow.

3.2. Generation and transmission of the ultrasonic pulses.

The ultrasonic measuring pulses were transmitted by a small condenser transmitter of a type which was developed at the III. Physikalisches Institut of the University of Göttingen [10]. The radiating diaphragm of this condenser transmitter has a diameter of 1.2 cm and consists of a thin styroflex-foil (10^{-3} cm thick) which is metallized on one side. Its other side lies straight on a metallic back plate which has concentric grooves in order to get a suitable air cushion between the diaphragm and the rigid back plate. A detailed construction drawing of this transmitter is included in [11]. This type of transmitter is well applicable for the transmission of pulses of ultrasonics into air, because it has a high natural frequency (about 200 kcps) and is highly damped, the latter property being the reason for a wide usable frequency response.

The voltages which are necessary in order to drive the sound transmitter were generated by the "generator of pulsed oscillations" (see fig.2), the circuit diagram of which is given in fig.4. By this circuit a sine wave (U 1 in fig.3) which is connected to IN-1 is gated in the following manner: The circuit stages belonging to the tubes T 1 to T 4 are parts

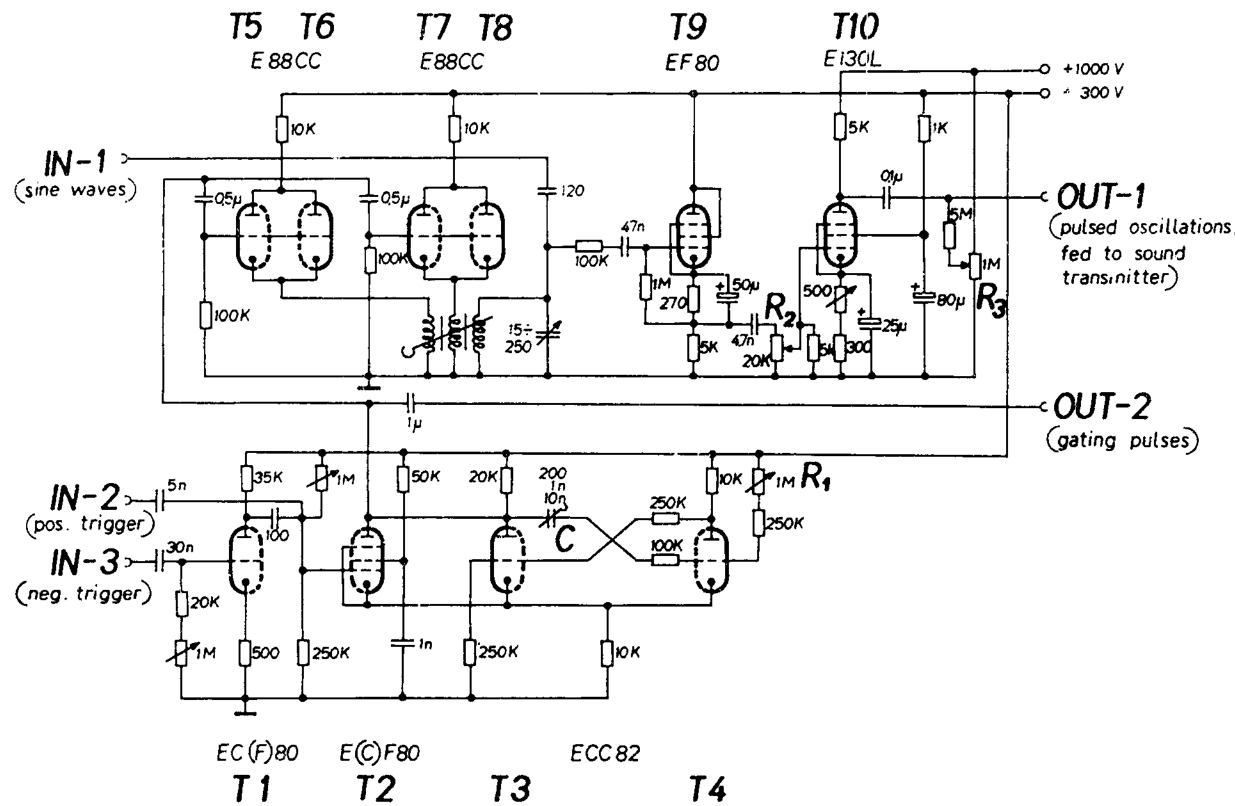

Fig.4: Circuit diagram of the "generator of pulsed oscillations" (see fig.2).

of a monostable multivibrator ("gating pulse generator" in fig.2), which is triggered by positive-going voltage steps occuring at IN-2 (or by negative-going voltage steps occuring at IN-3, respectively). By this multivibrator negative gating pulses (U 3) were generated, the repetition frequency of which was equal to the repetition frequency of the triggering clock pulses (U 2) (the "clock pulse generator" was an oscillator delivering rectangular waves of variable frequency). The duration of the gating pulses could be adjusted by C and R_1. The gating pulses are fed to the control grid of the four tubes T 5 to T 8 , which are coupled two by two in parallel in order to increase the transconductance. The cathode impedance of each of the two pairs of tubes which are controlled by the gating pulses consists of a coupling-coil; both the coupling coils are wound on one and the same iron core together with the inductivity of a parallel resonant circuit. The oscillatory circuit is tuned to the frequency of the sine waves which are connected to IN-1. If a current is just flowing through the tubes T 5 to T 8, the oscillatory circuit is highly damped by the low cathode impedances of the tubes, and at its upper end (the lower one is grounded) practically no voltage is obtained. But if suddenly the plate currents of the tubes are blocked by a negative gating pulse, the cathode impedance which is transformed into the resonant circuit is very high and causes only very small damping of the circuit. In this case at its upper end one gets nearly the full scale voltage which is present at IN-1.

If the damping of the oscillatory circuit during the interpulse intervals would be made by one of the two pairs of tubes only (T 5, T 6 or T 7, T 8), a voltage step would be transmitted into this circuit, too. This would excite damped oscillations in the natural frequency of the oscillatory circuit, which, in general, would superpose irregularly on the oscillations which are forced from outside. In order to avoid this, the coupling coils of the two pairs of tubes are wound against one another. Thus, the effects the voltage

steps occuring at the cathodes of the tubes have on the oscillatory circuit compensate for each other. The damping which is desired is doubled by this method (in comparison to the damping which would be caused by one pair of tubes).

The pulsed oscillations which are generated by this method pass a cathode-follower. Its output is connected to a potentiometer, by which the pulse height can be varied. At last, in the last tube T 10, the pulsed oscillations are amplified to a high voltage (up to about 400 V_{PP}) and, by a coupling condenser, are connected to the condenser transmitter. In addition, the condenser transmitter is supplied with a high voltage d-c bias (1000 V in maximum), which is adjustable by R_3. Both voltages which drive the condenser transmitter are adjusted for maximum undistorted sound radiation, the sum of the two voltages being limited by the puncturing voltage of the styroflex diaphragm.

The diaphragm of the condenser transmitter during the measurements in turbulent flow is exposed to certain fluctuations of pressure which are due to the turbulence of the flow. On principle, these fluctuations cause the diaphragm to be pressed on the back plate more or less. If this effect would be strong enough, corresponding fluctuations of the sensitivity of the transmitter system would be produced, which would give rise to undesired fluctuations of the measuring voltage. An experimental investigation and an estimate (both are reported in the appendix, Section 6.2.) led to the result, that this effect is too small for disturbing the measurements.

3.3. Reception and measurement of the ultrasonic pulses.

The measuring pulses are received by a condenser microphone which is designed identically to the sound transmitter (see Section 3.2.). This microphone is connected to a preamplifier, the circuit diagram of which is shown in fig.5. It has a high input impedance for the microphone and

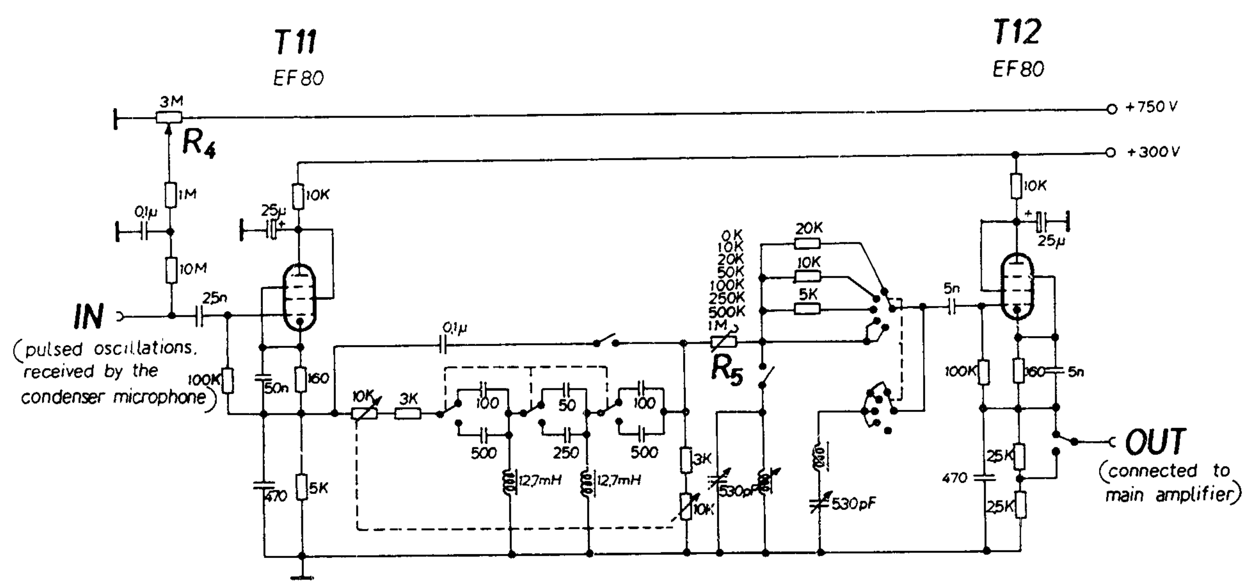

Fig.5: Circuit diagram of the "microphone preamplifier" (see fig.2).

additionally, supplies it with a positive d-c bias (the bias voltage can be adjusted by the potentiometer R_4). The first stage of the amplifier is an impedance matching cathode-follower, the low impedance output of it being connected to a high pass filter. The cutoff frequency of this filter can be switched over from 50 kcps to 110 kcps, and its input- and output-impedance is adjustable to an optimum. The high pass filter is followed by a parallel resonant circuit which is tuned to the measuring frequency. Its bandwidth can be varied by R_5 . Separated by a switchable decoupling resistor, a series resonant circuit, acting as an acceptor circuit, is connected in parallel to the parallel resonant circuit. Using all possibilities of adjustment, one can obtain an optimal adjustment of the filters with regard to the suppression of acoustically received disturbances: The high pass filter on the whole suppresses the low frequency noise, the parallel resonant circuit selects the measuring frequency from high frequency noise, and the absorber circuit, in addition, serves for the damping of small bandwidth disturbances which might be due to the production of turbulence by grids.

The voltage which is obtained at the end of the filter set (U 5 in fig.3) passes through a second cathode-follower and then reaches the input of the main amplifier, the circuit diagram of which is to be seen in fig.6. It is amplified by the first and the second stage (T 13 and T 14) of this amplifier. At the input of the third stage a time selection is applied; it only leaves the middle part of the directly received pulses unchanged and short-circuits all other parts of the voltage, including the swinging in and the swinging out part of the directly received measuring pulses and all reflected pulses. The circuit of the auxiliary circuit which is needed for this time selection ("selecting unit for measuring pulses" in fig.2) is shown in fig.7 (it was designed according to data taken from [12]). Its function is as follows: If the tube T 17 is in the cut-off condition, a current flows through the vacuum tube diodes T 18 and T 19

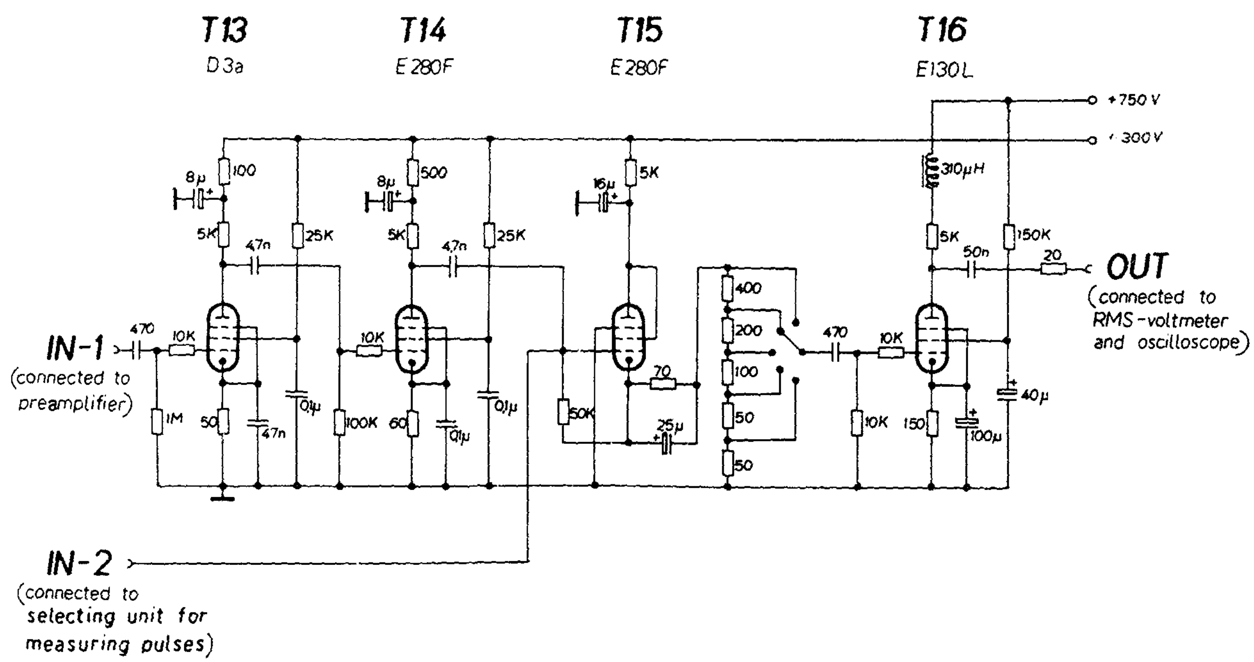

Fig.6: Circuit diagram of the "main amplifier" (see fig.2).

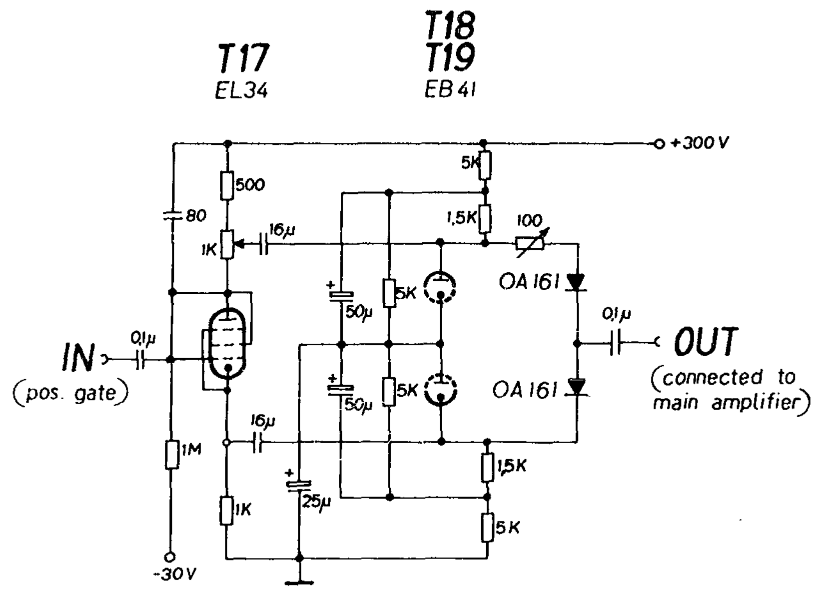

Fig.7: Circuit diagram of the "selecting unit for measuring pulses" (see fig.2).

and through the two semiconductor diodes OA 161. In this case the diodes act as a short-circuit with regard to the alternating current which is present at the grid of T 15 . If, however, T 17 is opened by a positive selecting pulse[1] (U 7 in fig.3), the diodes are blocked by the rectangular pulses occuring at the anode and the cathode of T 17 , thus interrupting the short-circuit of the alternating current at the grid of T 15 for the time t_2 . The selected measuring pulses (U 8 in fig.3) are amplified to a high voltage (400 V_{PP} in the maximum) by the last amplifier stage (T 16) and are fed to a rms voltmeter and to an oscilloscope.

[1] Positive selecting pulses of adjustable length t_2 and delay $\tau_1 + \tau_2$ against the corresponding clock pulses are obtained from the "selector pulse generator" (see fig.2) (type 161 pulse generator from Tektronix) in connection with a "pulse delaying unit" (type 162 waveform generator from Tektronix).

For the measurement of the rms voltage of the pulsed oscillations U 8 , which, in addition, sometimes are modulated by up to 100 percent, a voltmeter came into question only, the rms value indication of which is absolutely independent of the curve shape of the voltage within the range of ultrasonic frequencies used. The measurements were, therefore, partly performed by a thermo-junction in connection with a reflecting galvanometer. Occasionally, this arrangement had the disadvantage that the fluctuations of the voltage occuring statistically were not sufficiently suppressed by the damping of the measuring system. In addition, the thermo-junction which is very sensible against overloads was often damaged, if the diaphragm of the receiving microphone was punctured (this, in general, leading to no further effect). Later on, from this reason, the measurements were performed by an electrostatic voltmeter with spot light indication, which was furnished with an oil damping adjustable within wide limits. This instrument was not affected by overloads.

If one has measured the rms value of the output voltage of the condenser microphone (in arbitrary units), taking into account the directly received sound pulses only, one obtains the sound intensities I^{lam}_{meas} and I^{turb}_{meas} by squaring the measured values. From these values, one finds the damping ΔI as described in Section 3.1.

The received measuring pulses were observed by an oscilloscope (type 545 from Tektronix), mainly in order to check and to adjust the apparatus. Additionally, by use of the amplitude discriminator which is contained in the oscilloscope, measurements of a prevailing modulation frequency could be obtained from the scope. For this purpose the triggering level of the sweep of the oscilloscope was adjusted to such a value, that only the highest maxima of the voltage started a single sweep. By this method, each single scope pattern began with a maximum of the modulation of the alternating voltage, and, if a prevailing modulation frequency was present, the next following maximum of the modulation could be observed on the

scope, too. The difference in time between these maxima could be measured; it is equal to the duration τ_M of one cycle of the modulating voltage.

4. Performance of the measurements of the scattering of sound and evaluation of the results.

4.1. Damping of sound caused by turbulent scattering as a function of the turbulent fluctuation velocity and of the sound frequency.

In the figures 8 to 15 the results of measurements of the damping ΔI are presented, which were obtained with turbulence producing grids varying in M and D (meshlength and diameter of the rods) at different distances d from the grid. For each arrangement of the grid either the dynamic pressure q of the main flow or the sound frequency ν or both together were varied. The measurements were performed by use of the method described in Section 3.1. Each measuring point which is drawn into the figures represents the average value of the results of five single measurements (or more, in some cases).

At first fig.8 shows a series of measurements, in which only q was varied. As is to be seen, ΔI increases linearly with q over a wide range of q . The dynamic pressure, as is well known, is proportional to the square of the main flow velocity U , which, on the other hand, produces a fluctuation velocity u' proportional to U behind the turbulence grid. Therefore, the results presented in fig.8 prove the relation $\Delta I \sim u'^2$ to be valid. Instead of u' the nondimensional value $\frac{u'}{a_o}$ can be taken as a characteristic value of turbulence. Hence, one can write:

$$\Delta I \sim \left(\frac{u'}{a_o}\right)^2 \quad , \tag{20}$$

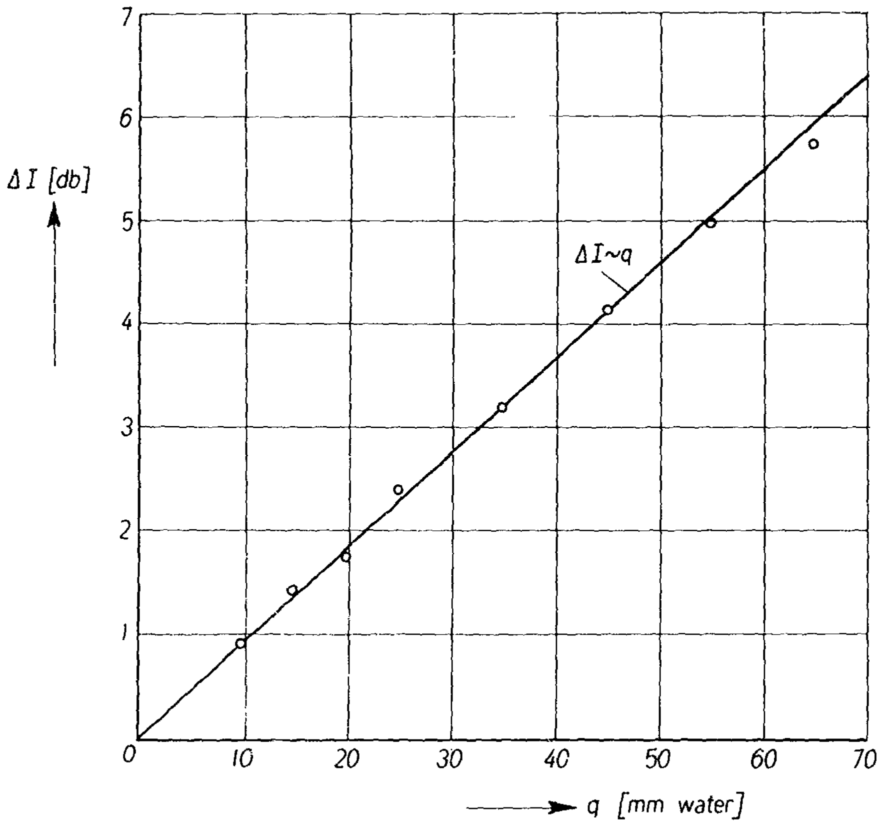

Fig.8: Damping Δ I of sound vs. dynamic pressure q of the main flow.
Data of the tests: s = 30.0 cm; ν = 200 kcps;
D = 1.00 cm; M = 2.59 cm; d = 21.0 cm.

that means, the scattering of sound by turbulence is proportional to the square of the Mach number of the turbulent fluctuation velocity. This experimental result is the same one as that derived theoretically (see Section 2.), if one makes the appropriate assumption, that the mean Mach number $\overline{M}$ of the scattering vortices, which was defined theoretically, is equal to the Mach number of the turbulence $\frac{u'}{a_o}$ except for a constant factor in the order of 1.

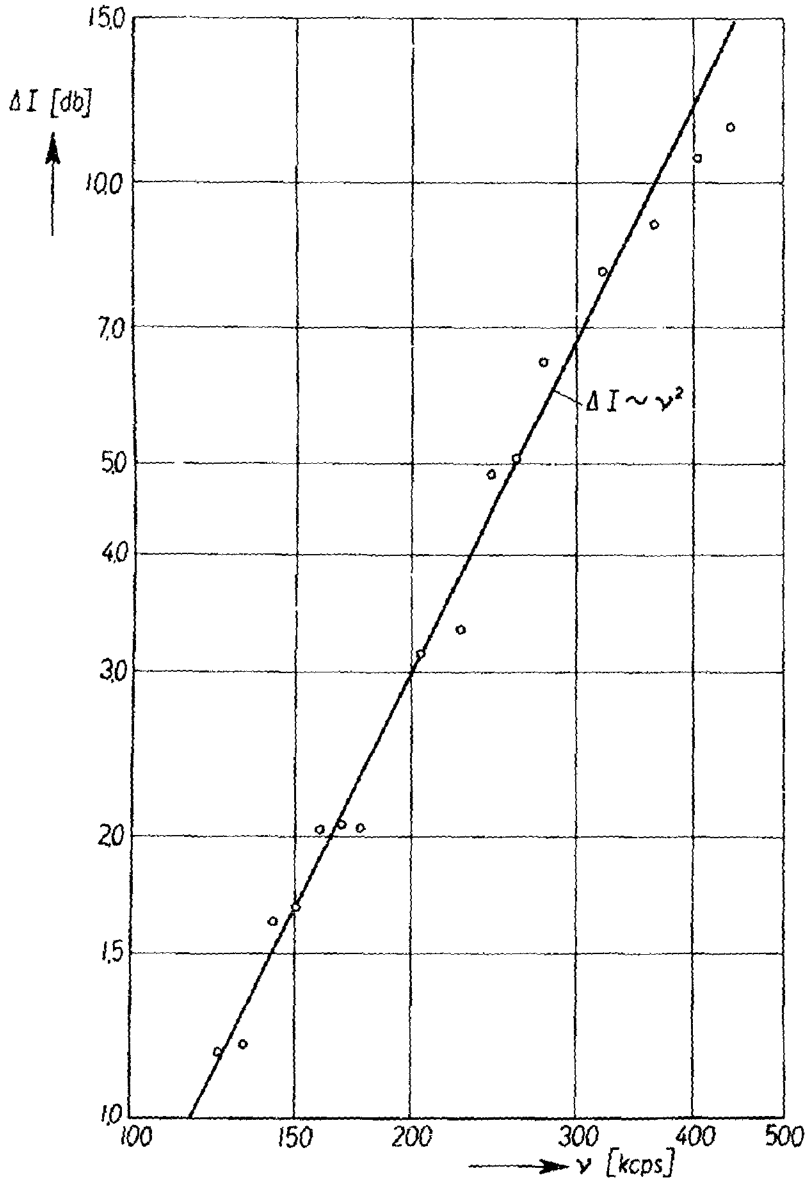

Fig.9: Damping ΔI of sound vs. frequency of sound. Data of the tests: s = 30.0 cm; q = 33 mm water; D = 0.25 cm; M = 1.28 cm; d = 7.0 cm. (This series of measurements exceptionally was performed with a square mesh grid.)

Fig.9 shows the results of a series of measurements, in which only the sound frequency ν was varied. The turbulent properties of the flow were held constant. The results of these measurements are represented by the relation

$$\Delta I \sim \nu^2 \tag{21}$$

over a wide range of ν . This result is in agreement with the theoretical prediction for large values of $R_a = \frac{r_a}{a_0} \cdot \nu$, r_a being the radius of the scattering vortices and ν being the frequency of sound. In this series of measurements r_a was roughly 0.3 cm (if one assumes r_a to be of the order of L_n). According to the lowest measuring frequency of ν = 130 kcps, the smallest value of R_a which was reached by these measurements was $R_a \approx 1.1$. Thus, the increase of the damping ΔI proportional to the square of the sound frequency ν , which was predicted theoretically for the case of large radii of the turbulent eddies and high frequencies of sound, is well confirmed by the measurements.

In fig.10 the results of a further series of measurements are to be seen, which were obtained by varying the dynamic pressure q of the mean flow as well as the sound frequency ν : In this case both relations (20) and (21) are represented together by the formula

$$\Delta I \sim q \cdot \nu^2 \sim \left(\frac{u'}{a_0} \cdot \nu\right)^2 , \tag{22}$$

which is well confirmed by the linear increase of ΔI plotted vs. $q \cdot \nu^2$.

In the range of smaller values of $R_a = \frac{r_a}{a_0} \cdot \nu$, measurements were carried out by reducing the dimensions of the scattering vortices. This was done by reducing the mesh-length M of the grid, the diameter D of the rods and the distance d between the grid and the sound beam as much as possible. The results of measurements, which were obtained in

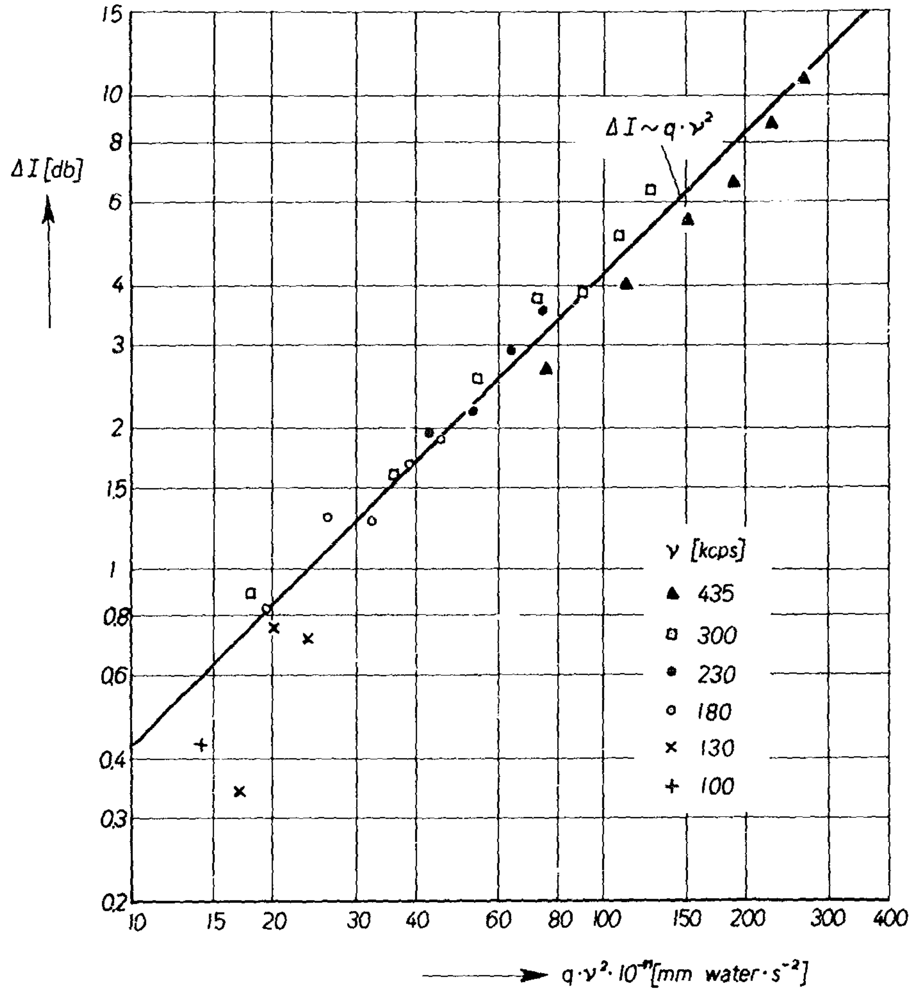

Fig.10: Damping ΔI of sound vs. the product of the dynamic pressure q of the main flow and the square of the sound frequency ν .
Data of the tests: s = 30.0 cm; D = 0.15 cm;
M = 2.50 cm; d = 5.0 cm.

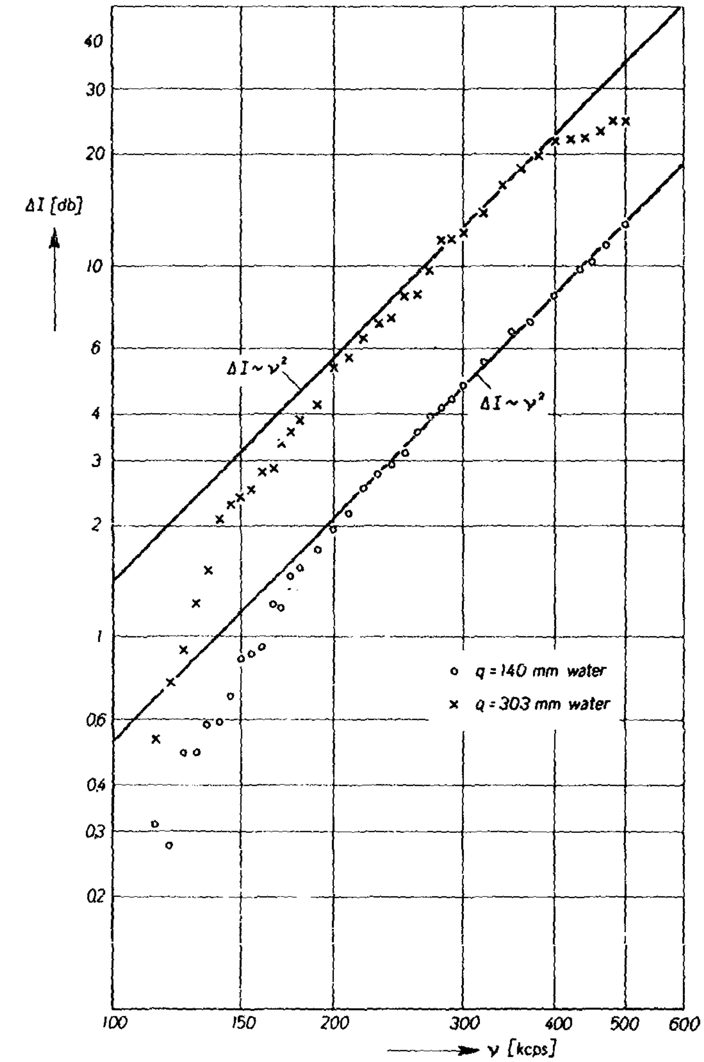

Fig.11: Damping ΔI of sound vs. frequency of sound in the transition region between the asymptotic power laws $\Delta I \sim \nu^2$ and $\Delta I \sim \nu^5$.
Data of the tests: s = 30.0 cm; D = 0.10 cm; M = 0.50 cm; d = 5.0 cm.
(The lines are the asymptotes in the ν^2-region.)

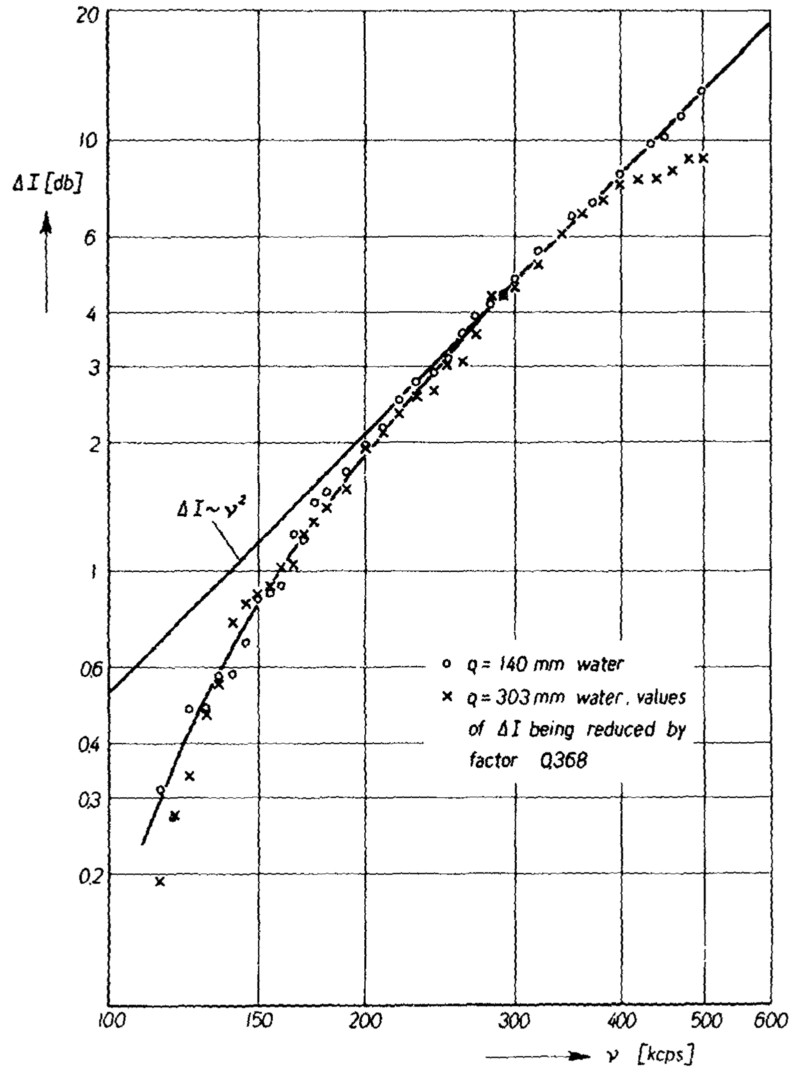

Fig.12: Same as fig.11, but upper curve shifted so far that it coincides with the lower one.
Data of the tests: s = 30.0 cm; D = 0.10 cm;
M = 0.50 cm; d = 5.0 cm.

this way, are plotted in fig.11: Two series of measurements, differing from one another in q by nearly the factor 2, were performed with the same grid. At high values of ν again the ν^2-law is confirmed by the measurements, except of a deviation in the case of very high values of ν at the greater q-value (the cause of which will be discussed more particularly below). In the range of lower sound frequencies, however, ΔI rises with a higher power of ν than with the second one. Evidently, this measured response comes from the transition between the asymptotic ν^2-law for high values of R_a and the asymptotic ν^5-law for small R_a-values, as theoretically predicted.

Applying the method described in Section 2., one can obtain informations about the values of r_a and $\overline{M}$ (which appear in the theory [1]) from this response. According to the theoretical results given in Section 2., the function $\Delta I = f(\nu)$ can be assumed to be the same one for both series of measurements which are plotted in fig.11, except of a constant factor. For the purpose of more exact graphical determination of the curve of this function, the upper series of measurements (belonging to the greater value of q) was brought to coincidence with the lower one by shifting it parallel to the ΔI-direction as far as was needed to obtain coincidence of the ν^2-asymptotes. (The amount of this shift was somewhat greater than would be expected according to the ratio of the two q-values. This probably is because of the higher value of q for which $\left(\frac{u'}{a_o}\right)^2$ is no longer exactly proportional to q.) Thus, one gets fig.12, in which the scale in ΔI is valid only for the measurements made at the smaller q-value. By application of equation (16), the frequency $\nu_{R_a=1} = 132$ kcps was deduced from the curve in this figure. Hence, from (17) and (18), the following values of r_a and $\overline{M}$ are obtained:

$$r_a = 0.26 \text{ cm}$$
$$\overline{M} = 6.2 \cdot 10^{-3}\ .$$

This lies well in the order of magnitude expected.

The deviation from the ν^2-law at the right end of the upper curve in fig.11 gave the impulse to further investigations at higher values of $\frac{u'}{a_o} \cdot \frac{L_n}{a_o} \cdot \nu$, which correspond to high values of $\overline{M} \cdot \frac{r_a}{a_o} \cdot \nu$ in the theory. As was mentioned above, the theoretical results are valid with the assumption of not

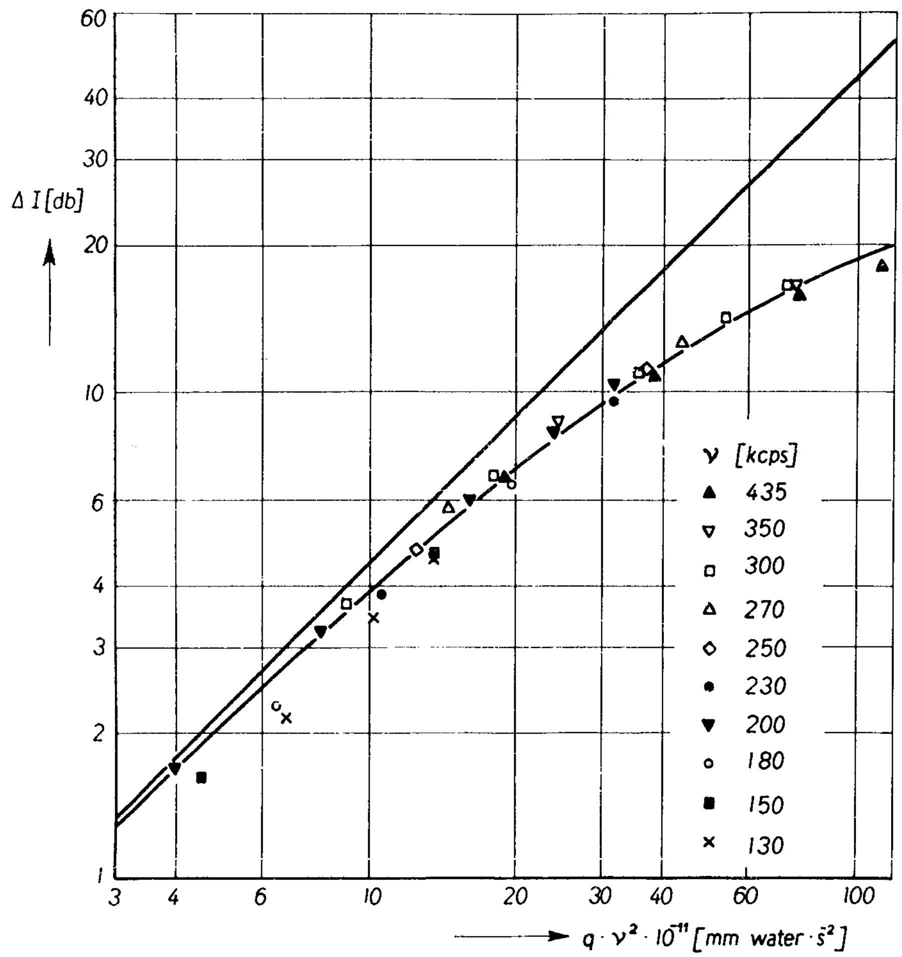

Fig.13: Damping ΔI of sound vs. the product of the dynamic pressure q of the main flow and the square of the sound frequency ν.
Data of the tests: s = 30.0 cm; D = 1.00 cm; M = 2.50 cm; d = 20.0 cm.

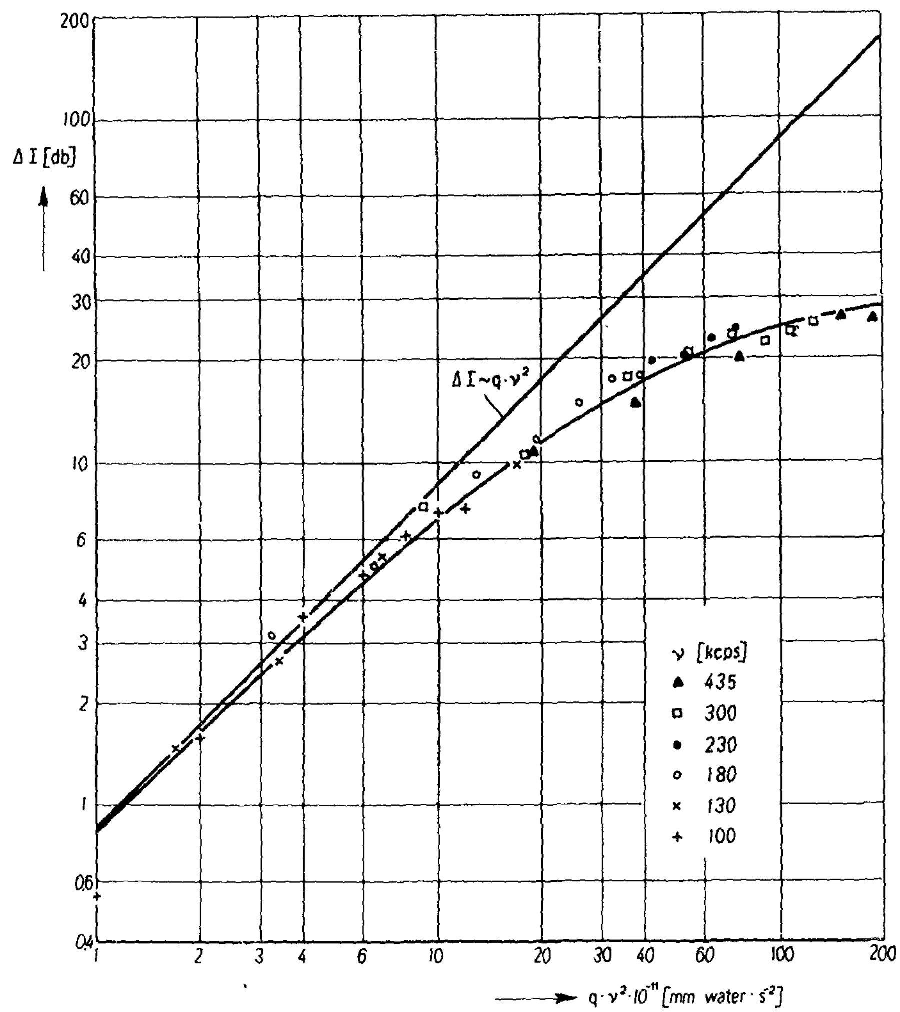

Fig.14: Damping ΔI of sound vs. the product of the dynamic pressure q of the main flow and the square of the sound frequency ν .
Data of the tests: s = 30.0 cm; D = 0.40 cm;
M = 2.50 cm; d = 5.0 cm.

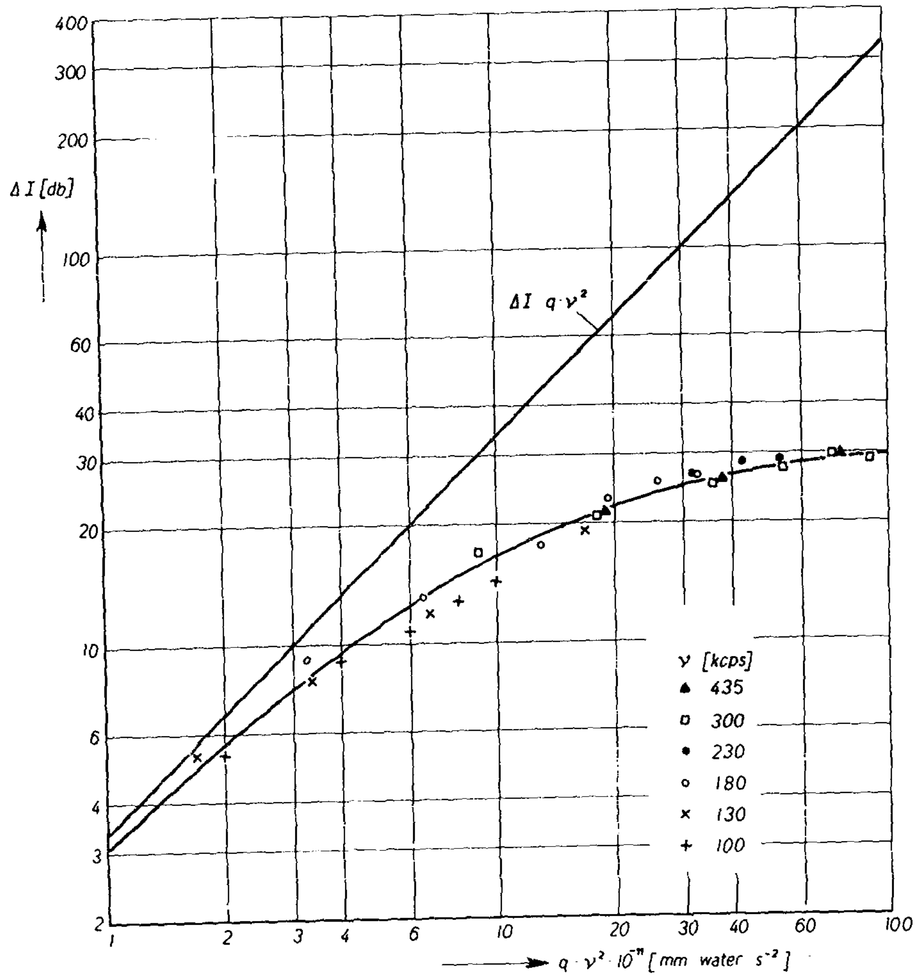

Fig.15: Damping ΔI of sound vs. the product of the dynamic pressure q of the main flow and the square of the sound frequency ν .
Data of the tests: s = 30.0 cm; D = 1.00 cm; M = 2.50 cm; d = 5.0 cm.

too large values of $\overline{M}\cdot\frac{r_a}{a_o}\cdot\nu$ only; hence, it seemed to be possible, that at higher values of $\overline{M}\cdot\frac{r_a}{a_o}\cdot\nu$ or $\frac{u'}{a_o}\cdot\frac{r_a}{a_o}\cdot\nu$, respectively, the dependence of ΔI deviates from the law $\Delta I \sim (\overline{M}\cdot\nu)^2$ or $\Delta I \sim (\frac{u'}{a_o}\cdot\nu)^2 \sim q\cdot\nu^2$, respectively.

In order to answer this question, three further series of measurements were performed under different turbulent conditions. The results are presented in the figs.13 to 15 : In fig.13 and 14 the measuring points at smaller values of $q\cdot\nu^2$ still follow the function $\Delta I \sim q\cdot\nu^2$, which was confirmed above already. At higher $q\cdot\nu^2$-values, however, ΔI increases slowlier. In the case of the measurements plotted in fig.15 even the whole curve ΔI vs. $q\cdot\nu^2$ increases slowlier than linear with $q\cdot\nu^2$.

The results of measurements which are plotted in figs.13 to 15 at first were approximated by curves (not being drawn here), which, for their part, were approximated by a development into Chebyshef's polynomials and into power series. On the basis of these computations, the following single function was suggested to represent all three series of measurements:

$$\Delta I = C_1\cdot\frac{C_2\cdot q\,\nu^2}{1+C_2\cdot q\,\nu^2} \quad . \qquad (23)$$

The coefficients C_1 and C_2 had the following values in the three series of measurements:

Meas. of fig.13: $C_1=32.2$; $C_2=1.40\cdot10^{-13}$ s^2/mm water ,

meas. of fig.14: $C_1=34.3$; $C_2=2.51\cdot10^{-13}$ s^2/mm water ,

meas. of fig.15: $C_1=32.8$; $C_2=1.04\cdot10^{-12}$ s^2/mm water .

The curves which were obtained inserting these values of C_1 and C_2 in equation (23) are to be seen in the figures; obviously, the measurements are well represented by them.

4.2. Dependence of the turbulent damping on the distance covered by the sound waves within the turbulent medium.

Directly behind a grid consisting of parallel rods, as it was used for the generation of turbulence in the measurements, a region exists in which the single turbulent wakes behind the rods are still separated from one another by regions of laminar flow. If sound waves are transmitted through this region the length s of the sound path in turbulent flow is proportional to the number n of the wakes which is proportional to $\frac{1}{M}$ (where M is the meshlength of the grid). In some distance d_z from the grid the wakes grow together. From data presented in [13] the following estimation formula for d_z can be deduced:

$$d_z = 1.1\ D\ (0.925 \cdot \frac{M^2}{D^2} - 1) \quad . \qquad (24)$$

Hence, if this relation is maintained, the following relation applies:

$$s \sim n \sim \frac{1}{M} \quad . \qquad (25)$$

This simple relation between s and n or M, respectively, was the basis for direct measurements of the dependence of the damping ΔI on s. Varying M only in the way described, one can assume, that the turbulent quantities L_n (macroscale) and $\frac{u'}{a_o}$ (Mach number of the fluctuation velocity) remain constant, if the dynamic pressure q of the mean flow is held constant. Thus, at a constant frequency ν of the sound the value of $\frac{u'}{a_o} \cdot \frac{L_n}{a_o} \cdot \nu$ remains constant, too, so that ΔI can be expected to be dependent on s only.

The results of two series of measurements which were obtained by the method of measurement described are plotted in fig.16: The measuring points for which the relation $d \lesssim d_z$ held are drawn as full circles, all other measuring points as open circles. The first ones are represented very well by the

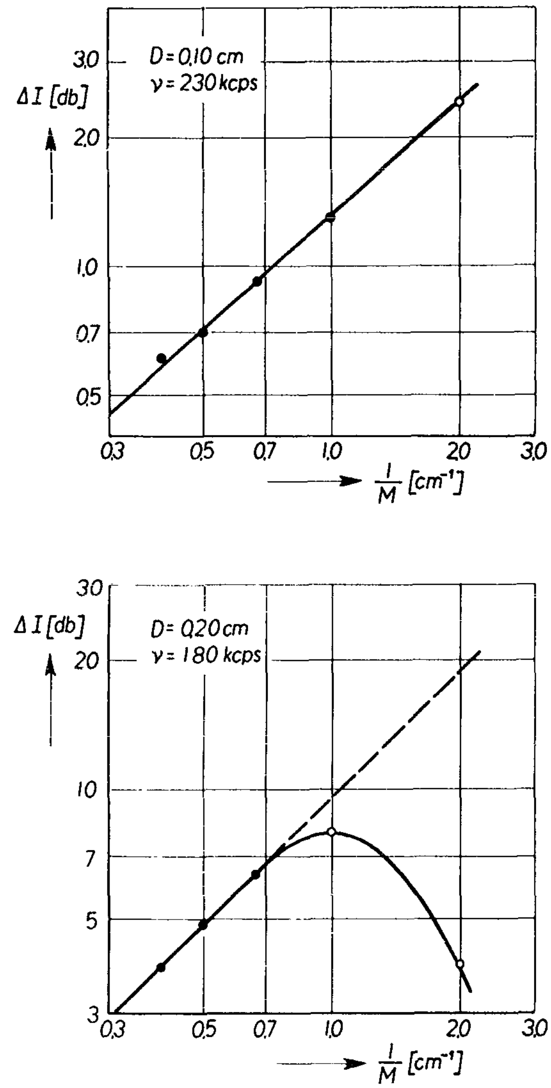

Fig.16: Dependence of the turbulent damping ΔI on the meshlength M of the turbulence producing grid. Data of the tests: s = 30.0 cm; q = 100 mm water; d = 5.0 cm.

simple law $\Delta I \sim \frac{1}{M}$ or, according to relation (25), by

$$\Delta I \sim s \quad . \tag{26}$$

This result confirms well the expected and (for not too large values of $\frac{u'}{a_o} \cdot \frac{L_n}{a_o} \cdot \nu$) predicted dependence of the damping ΔI on s (see Section 2.).

The decrease of ΔI at high values of $\frac{1}{M} \sim n$, as is to be seen in the case of thicker rods (D = 0.2 cm) , corresponds to measurements only, for which already $d \gtrsim d_z$. In this region strong interactions between the single turbulent wakes take place, which make the determination of the turbulent quantities somewhat difficult. Hence, the damping ΔI in this range shall not be regarded here.

At greater values of $\frac{u'}{a_o} \cdot \frac{L_n}{a_o} \cdot \nu$ the measurements described above were repeated with thicker rods (D = 1.0 cm). Moreover, the dependence of ΔI on s was determined by another method: The receiving microphone was stepwise shifted closer to the sound transmitter, a procedure by which s was varied more directly than before; all other conditions were kept constant, especially the arrangement of the grid and the velocity U of the main flow. The results of these measurements could approximately be represented by the formula

$$\Delta I = K_1 \cdot \frac{K_2 \cdot s}{1 + K_2 \cdot s} \quad . \tag{27}$$

For one special grid (M = 2.50 cm; D = 1.00 cm; d = 5.0 cm) the following values of K_1 and K_2 were obtained:

$$K_1 = 41.9$$

$$K_2 = 7.9 \cdot 10^{-2}\ \mathrm{cm}^{-1} \ .$$

4.3. Dependence of the scattering of sound on the angle between a prevailing direction of the scattering vortices and the direction of sound propagation.

The turbulence which is produced by a grid consisting of parallel rods (as was the case for nearly all measurements given here) is strongly non-isotropic in such a manner that, shortly behind the grid, the axes of the turbulent

eddies have a predominant direction parallel to the rods. In a series of measurements the results of which are presented in fig.17 the dependence of the sound damping ΔI on the angle between the predominant direction of the vortex axes and the direction of sound propagation was investigated.

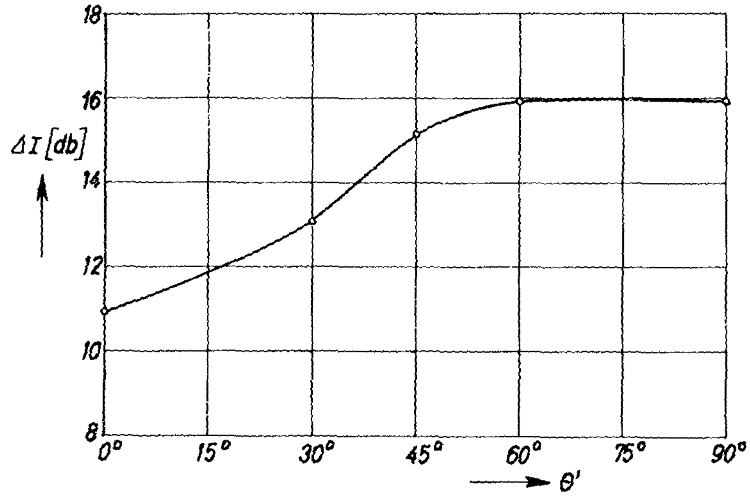

Fig.17: Dependence of the turbulent damping ΔI on a predominant direction of the scattering vortices (θ' = angle between the rods of the turbulence grid and the direction of wave propagation).
Data of the tests: $s = 30.0$ cm; $q = 42$ mm water; $\nu = 220$ kcps; $D = 0.50$ cm; $M = 1.28$ cm; $d = 12.0$ cm.

As one sees from the figure, the damping ΔI has a minimum at $\theta' = 0^o$ and reaches a maximum at $\theta' \approx 90^o$, where θ' is the angle between the rods of the grid and the direction of wave propagation. At small values of θ' the sound waves predominantly pass through the vortices in vortex axis direction, at values near 90^o perpendicular to it. Between these extreme values ΔI increases monotonously. This dependence of ΔI on θ' is qualitatively equal to the dependence of ΔI on θ, which was deduced theoretically for the case of extreme non-isotropy (see formula (4)). Of course,

ΔI cannot become zero at $\theta' = 0^{\circ}$, because, according to the transition of the wake flow turbulence from non-isotropy to isotropy, in the path of the sound waves vortices are present with axis directions differing from the direction of the rods.

4.4. Modulation of the sound amplitude due to scattering by vortices following one another almost periodically.

The wake flow behind a single circular rod which is mounted perpendicular to the flow direction consists of vortices periodically following one another (v.Kármán vortex street), if the Reynolds number $Re = \frac{D \cdot U}{\nu_a}$ is smaller than 150 (D = diameter of the rod, U = main flow velocity, ν_a = kinematic viscosity of air). These vortices are generated by alternating separation of the flow at both sides of the rod. The frequency of this separation (the "shedding frequency") at each side is given by

$$n_1 = S \cdot \frac{U}{D} \quad , \qquad (28)$$

where S is the Strouhal number (see, for instance, [14]). At not too great a distance from the rod this frequency of vortices remains predominant even if, at increased Reynolds numbers, the vortex street changes to a turbulent wake. In the frequency spectrum of the turbulence this discrete frequency is to be seen as a peak which overtops the continuous part of the spectrum. At such high values of the Reynolds number ($Re \gtrsim 300$) the Strouhal number S has the constant value 0.212. Because vortices are generated alternatingly at both sides of the rod with the frequency n_1, a second discrete frequency $n_2 = 2\,n_1$ can be distinguished in the frequency spectrum at a distance sufficiently close to the rod. It was to be expected, that these predominant frequencies of the vortices would be identifiable in the amplitude modulation which is impressed on sound by scattering if it runs through such a turbulent wake. This expectation was verified by a series of measurements in

the following way:

Instead of the grid of parallel rods used for the production of turbulence until now, a single rod was inserted into the flow at a distance $d = 5$ cm from the sound beam. Its diameter was $D = 0.4$ cm in one case and $D = 0.6$ cm in another one, and the sound frequency was 230 kcps. The observation of the received sound by an oscilloscope (see Section 3.3.) yielded a typical pattern a sketch of which is shown in fig.18; as is seen from it, two predominant frequencies of the modulation can be distinguished distinctly, which have a ratio of 2 : 1 . The lower one was determined by measuring the duration τ_M of one period.

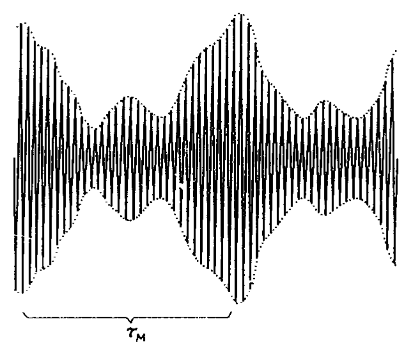

Fig.18: Sketch of a typical scope pattern of sound waves which are modulated by scattering due to v.Kármán vortices in the wake flow of a cylinder.
τ_M : duration of one period of modulation.

The results of these measurements are presented in table 1 and are compared with the shedding frequencies calculated by (28). Within the accuracy which could be obtained by this simple method of measurement the modulation frequency n_{M_1} which was measured agrees well with the shedding frequency n_1, and the second frequency n_{M_2} with n_2 , correspondingly.

The investigations show that the v.Kármán vortices which are still identifiable in the turbulent wake flow behind a

circular rod may have a considerable influence on the scattering of sound.

D [cm]	U $[cm \cdot s^{-1}]$	τ_M [ms]	n_{M_1} [kcps]	$n_1 = S \cdot \frac{U}{D}$ [kcps]
0.4	$1.81 \cdot 10^3$	1.00	1.00	0.96
	$2.56 \cdot 10^3$	0.80	1.25	1.36
	$3.14 \cdot 10^3$	0.64	1.56	1.66
	$3.62 \cdot 10^3$	0.56	1.79	1.92
	$4.05 \cdot 10^3$	0.50	2.00	2.15
	$4.44 \cdot 10^3$	0.46	2.18	2.35
	$4.79 \cdot 10^3$	0.42	2.38	2.54
0.6	$2.56 \cdot 10^3$	1.20	0.83	0.90
	$3.14 \cdot 10^3$	1.00	1.00	1.11
	$3.62 \cdot 10^3$	0.92	1.09	1.28

<u>Table 1</u>: Measurements of the predominant frequency of sound wave modulation which is caused by turbulent scattering within the wake flow of a cylinder; comparison with the shedding frequency of v.Kármán vortices.
Sound frequency $\nu = 230$ kcps; distance between the cylinder and the sound path $d = 5.0$ cm;
τ_M : measured duration of one period of modulation; $n_{M_1} = 1/\tau_M$:modulation frequency; n_1 : shedding frequency (calculated); $S = 0.212$: Strouhal number.

5. Deduction of a general formula for the damping of sound by turbulence. Application to the attenuation of sound in the free atmosphere.

From the theory [1] the formula (4) was obtained (see Section 2.) for the damping of sound due to scattering by extremely non-isotropic turbulence (valid at $R_a = \frac{r_a}{a_o} \cdot \nu \gg 1$ and at not too great values $\overline{M} \cdot \frac{r_a}{a_o} \cdot \nu$). If in this formula R_a is replaced by $\frac{r_a}{a_o} \cdot \nu$, it reads for $\theta = 90^o$:

$$\Delta I = 80\, \pi^2 \left(1 - \frac{2}{\pi}\right) \cdot \log e \cdot \frac{s}{r_a} \left(\overline{M} \cdot \frac{r_a}{a_o} \cdot \nu\right)^2 \quad . \qquad (29)$$

The turbulence which, in the measurements performed, was produced by grids of parallel rods has turbulent properties which lie between the limiting cases of full isotropy and extreme non-isotropy. Because of a difference in the damping ΔI of only 21% between these two limiting cases (related to the case of isotropy) one can - without significant error - assume the formula (29) to be valid for the conditions, under which the measurements presented in Section 4. for $R_a \gg 1$ were carried out. Substituting the quantities r_a (radius of the vortices) and $\overline{M}$ (mean Mach number of the vortices), which were used in the theory, by the turbulent quantities L_n (macroscale perpendicular to the mean flow) and $\frac{u'}{a_o}$ (Mach number of the rms value of the fluctuation velocity), one obtains the following formula which is analogous to (29) and which holds for not too great values of $\frac{u'}{a_o} \cdot \frac{L_n}{a_o} \cdot \nu$:

$$\Delta I = k_1 \cdot \frac{s}{L_n} \left(\frac{u'}{a_o} \cdot \frac{L_n}{a_o} \cdot \nu\right)^2 \quad . \qquad (30)$$

The dependence of ΔI on ν , u' and s which is expressed by this formula has been checked and confirmed experimentally by the measurements presented in Section 4.

Moreover, the experimental investigations led to the result, that at great values of $\frac{s}{L_n}\left(\frac{u'}{a_o}\cdot\frac{L_n}{a_o}.\nu\right)^2$ the simple formula (30) is to be replaced by the following one:

$$\Delta I = k_1 \cdot \frac{s}{L_n}\left(\frac{u'}{a_o}\cdot\frac{L_n}{a_o}.\nu\right)^2 \cdot \frac{1}{1 + k_2\,\frac{s}{L_n}\left(\frac{u'}{a_o}\cdot\frac{L_n}{a_o}.\nu\right)^2} \cdot \qquad (31)$$

The formula (30) is included herein as a limiting case for small values of $\frac{s}{L_n}\left(\frac{u'}{a_o}\cdot\frac{L_n}{a_o}.\nu\right)^2$.

For the determination of the constant k_1 a greater number of measurements of ΔI has been evaluated, which were performed with various turbulence grids, that means under various turbulent conditions, and for which one could be sure, that the value $\frac{s}{L_n}\left(\frac{u'}{a_o}\cdot\frac{L_n}{a_o}.\nu\right)^2$ was small enough for the application of formula (30). From the single values obtained the mean value

$$k_1 \approx 280$$

was calculated.

For the evaluation of these measurements the following relations after [15] were used:

$$\left(\frac{U}{u'}\right)^2 \approx \frac{b}{3C_D}\left(\frac{d}{M} - \frac{d_o}{M}\right) \qquad (32)$$

$$L_p \approx 2\,L_n \approx 0.95\,M\,\sqrt{\frac{C_D}{b}}\,\sqrt{\frac{d}{M} - \frac{d_o}{M}}\;, \qquad (33)$$

where C_D is the drag coefficient of the turbulence grid, which was calculated from data in [16]. For b the value b = 53 was inserted, which (after [15]) is valid for grids consisting of parallel rods,and d_o/M was taken equal to 10 (after [15], too). Of course, only measurements were used for which the relation $d/M > 20$ held, for, only in this region (that means at sufficient great distances from the grid) the formulas (32) and (33) are valid. Additionally, it can be assumed, that the relation $L_p = 2\,L_n$, which holds for isotropic turbulence, is valid sufficiently exact at distances $d/M > 20$.

As was gathered from the literature concerning the measurement of turbulence behind grids (see, for instance,

[17 to 23]), the results obtained by other authors with square mesh grids of round bars partly differ considerably from the results presented in [15]. These latter results, however, were obtained in a wind tunnel with a particular low degree of wind tunnel turbulence, and, moreover, they include measurements behind such grids of parallel rods which were used for the present measurements. From these two reasons the data given in [15] were used for the evaluation of the sound damping measurements.

The coefficient k_2 in formula (31) was estimated in the following manner: In [24] the results of measurements of the longitudinal macroscale L_p of the turbulence in the wake flow of a circular rod are given at distances related to the diameter of the rod of $d/D = 80$; 120 and 160 . Under the assumption that L_p is approximately equal to $2\ L_n$ and proportional to the width of the wake which is computable by equation (35) (this latter assumption was checked by the values of L_p given in [24]) one obtains the following formula for L_p or L_n , respectively:

$$L_p \approx 2\ L_n \approx 0.25\ D \sqrt{1 + 0.92 \frac{d}{D}} \quad . \tag{34}$$

By this formula, L_n could be calculated in cases in which - in the region of the sound beam - the flow consisted of single wakes behind the rods, e.g. in the measurements shown in fig.14. The grid used there consisted of rods $D = 0.40$ cm in diameter and $M = 2.50$ cm distant from one another, and the distance between the grid and the sound beam axis was $d = 5.0$ cm . After [13] the following estimation formula holds for the width $2\ y_R$ of the wakes behind the rods:

$$2\ y_R \approx D \sqrt{1 + 0.92 \frac{d}{D}} \quad . \tag{35}$$

At the distance $d = 5.0$ cm one gets the value $2\ y_R = 1.47$ cm; thus it can be assumed, that the single wakes do not yet interact with one another. Under these circumstances the length s of the sound path within the turbulent medium can be put equal to the sum of the widths of the single wakes, that means, if n is the number of the wakes (which was equal to 12 in the case of fig.14),

$$s \approx n \cdot 2\ y_R = 12 \cdot 1.47 = 17.6 \text{ cm} .$$

L_n is estimated from formula (34) to be 0.177 cm. From that, at the end, a value of $\frac{s}{L_n} \approx 100$ is obtained. The values of L_n and $\frac{s}{L_n}$ thus being known, one can calculate the unknown constant k_2 by formula (31) inserting special pairs of values of ΔI and ν taken from fig.14 (with an arbitrary,

but constant value of q). Thus, one gets the following value:

$$k_2 \approx 8.1 \quad .$$

The experimental results obtained can be used to calculate the damping of sound due to scattering in the free turbulent atmosphere. The atmospheric turbulence has a structure similar to that shortly behind a grid of parallel rods (see the beginning of this section): One can assume, that the axes of the turbulent eddies have a predominant direction parallel to the surface of the earth and perpendicular to the direction of the wind. For the case which is of special interest, namely the scattering of aircraft-noise, one has air-to-ground propagation, that means propagation perpendicular to the surface of the earth. Further, the situation that the scattered sound is lost by sideward deflection is the same as in the experiments, for the aircraft noise has a distinct directivity pattern. Hence, the experimental results obtained above may be applied without restriction. Also for ground-to-ground propagation of sound the values given below hold well, because the scattering does not depend much on a predominant direction of the turbulent eddies, if the predominance - as is the case in the atmosphere - is not too distinct (see Section 4.3.).

An estimation given in [1] shows that in the free atmosphere damping due to scattering by turbulence becomes markable for $R_a = \frac{r_a}{a_o} \cdot \nu \gg 1$ only. Hence, in the range of ν which is of practical interest, one has to use equation (30) (if s does not become too large). Thus, the dependence of the damping ΔI per unit length on the sound frequency ν is given by

$$\frac{\Delta I}{s} = F \cdot \nu^2 \qquad \left[db \cdot m^{-1}\right] \quad , \qquad (36)$$

where the factor F is dependent on the turbulent quantities L_n (transversal macroscale) and u' (turbulent fluctuation velocity) which are just present in the atmosphere. Its value

has been calculated by formula (30) for different pairs of values of L_n and u' ; the results of these calculations are presented in table 2. [1] (Eventually, the damping calculated by formula (30) must be reduced due to formula (31) for large values of s or for very high frequencies ν of sound.)

u' [m]	L_n [m] 1	2	5	10	20	50
0.1	$2.0\cdot10^{-10}$	$4.0\cdot10^{-10}$	$1.0\cdot10^{-9}$	$2.0\cdot10^{-9}$	$4.0\cdot10^{-9}$	$1.0\cdot10^{-8}$
0.2	$8.0\cdot10^{-10}$	$1.6\cdot10^{-9}$	$4.0\cdot10^{-9}$	$8.0\cdot10^{-9}$	$1.6\cdot10^{-8}$	$4.0\cdot10^{-8}$
0.5	$5.0\cdot10^{-9}$	$1.0\cdot10^{-8}$	$2.5\cdot10^{-8}$	$5.0\cdot10^{-8}$	$1.0\cdot10^{-7}$	$2.5\cdot10^{-7}$
1.0	$2.0\cdot10^{-8}$	$4.0\cdot10^{-8}$	$1.0\cdot10^{-7}$	$2.0\cdot10^{-7}$	$4.0\cdot10^{-7}$	$1.0\cdot10^{-6}$

Table 2: Factor F of equation (36), calculated by equation (30). (Dimension of ν in eq.(36): cps .) L_n : lateral macroscale; u' : rms value of the turbulent fluctuation velocity.

Direct measurements of the damping of sound in the free atmosphere were performed by P.H. Parkin and W.E. Scholes [27] and led to a result which is represented by the following formula (ν measured in cps):

$$\frac{\Delta I}{s} = 2.5\cdot10^{-9}\cdot\nu^2 \quad [\mathrm{db\cdot m^{-1}}] \; . \tag{37}$$

This result shows that the damping is proportional to the square of the sound frequency (as in equation (36)), but because of the lack of exact informations about the turbulent conditions during their measurements it is not possible to say how far this damping is due to turbulent scattering.

1) After measurements performed by E.Frankenberger [25,26] L_n has values of 1 to 50 meters and u' is in the order of 0.1 to 1.0 meters per second in the lower atmosphere.

6. Appendix.

6.1. Investigation of the influence of turbulent pressure fluctuations on the sensitivity of the condenser microphones used.

As mentioned in Section 3.2. already, the sensitivity of the condenser microphones used in the experiments is changed if they are exposed to an outside positive or negative pressure. During the measurements the microphones are exposed to small pressure fluctuations which are due to the turbulent flow. It was guaranteed by the following investigations that such pressure fluctuations have no influence on the acoustical measurements performed.

The highest flow velocities applied in the measurements were about $U = 70\ \mathrm{m \cdot s^{-1}}$. The upper limit of the fluctuation velocity perpendicular to the diaphragms of the microphones was about $u'_{y\ max} \approx 10\ \mathrm{m \cdot s^{-1}}$ (corresponding to a maximum degree of turbulence of $(\frac{u'_y}{U})_{max} \approx 15\%$). This velocity $u'_{y\ max}$ generates a dynamic pressure of $q'_{max} \approx 6$ mm water $= 0.6\ \mathrm{p \cdot cm^{-2}}$.

The influence of low frequency pressure fluctuations of the order quoted on the transmission of the measuring pulses was investigated experimentally by a method outlined in fig.19: Both microphones which were used for the transmission and the reception of the ultrasonic measuring pulses were inserted in two opposite walls of an airtight box. As well as in the sound scattering experiments, sound pulses were transmitted and received. One of the solid walls of the box was substituted by the movable diaphragm of a loudspeaker. With the aid of this loudspeaker the air pressure in the box would be varied by $\pm$ 3 mm water according to the position of the diaphragm. The elongation of the diaphragm which was necessary for this variation could be calculated directly from the variations in volume and was $\pm$ 0.1 cm ; this value was to realize easily by proper voltages applied to the coil of the loudspeaker. If the loudspeaker is driven by an a-c voltage,

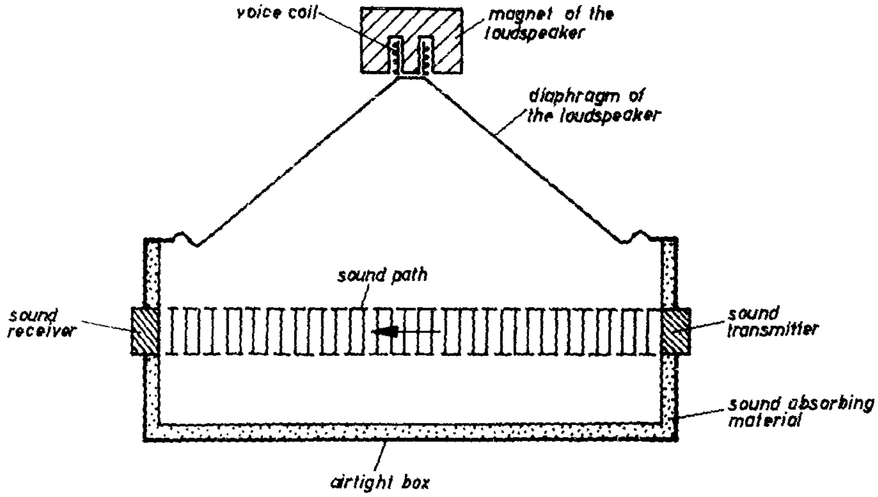

Fig.19: Sketch of the test setup used to check whether the sensitivity of the condenser microphones depends on turbulent pressure fluctuations.

the ultrasonic waves which were unmodulated before must be modulated, if an influence of the pressure fluctuations on the sensitivity of the condenser microphones exists. But no modulation could be observed even at greater fluctuations of the air pressure.

This negative result can be understood, if one calculates the electrostatic force by which the diaphragm of the microphone is pressed against the rigid back plate. The attraction between the two plates of a parallel plate condenser is given by

$$K = \frac{\varepsilon \cdot \varepsilon_0}{2} \cdot \frac{U_P^2 \cdot A}{\ell^2} ,$$

where U_P is the applied voltage, A is the area of the plate,

ℓ is the distance between the plates and $\varepsilon \cdot \varepsilon_o$ is the dielectric constant of the medium between the plates. For the microphones used the following numbers habe to be inserted: $U_p \approx 800$ V, $A \approx 0.5$ cm^2 (the part of the area of the diaphragm which covers the grooves of the back plate (see Section 3.2.) is not included in this value), $\ell \approx 10^{-3}$ cm, $\varepsilon = 2.3$ and $\varepsilon_o = 8.86 \cdot 10^{-14}$ $A \cdot s \cdot V^{-1} \cdot cm^{-1}$. From these values a force of 320 p is obtained which acts on the whole diaphragm; this force is due to a pressure of 280 $p \cdot cm^{-2}$ = 2800 mm water (related to the whole area of the diaphragm). This value exceeds the pressure fluctuations generated by the turbulence in the measurements by a factor of nearly 500. This estimate shows again, that no effect of the turbulent fluctuations on the ultrasonic measurements is to be expected.

6.2. Investigation of the influence of forward scattering on the measurements.

One speaks of "forward scattering" if the direction of the maximum intensity of the scattered sound deviates from the direction of propagation of the incident sound by a small angle only (see fig.4a in [1] for the case of $R_a = 10$, for instance). As was predicted by the theory, this effect can become markable with increasing frequency of sound. Because of the finite diameter of the sound beam and of the receiving microphone scattered sound which is generated in a certain region shortly before the receiving microphone may partly arrive at the diaphragm of the microphone. If these parts would exceed a certain intensity, they would cause errors of the measurements of the damping ΔI. In order to estimate the magnitude of this effect, a test was made in the manner sketched in fig.20:

In this test the turbulence producing grid consisted of a group of four rods, which made the flow turbulent only within a third of the cross section of the test duct. This group could be shifted in the direction parallel to the axis

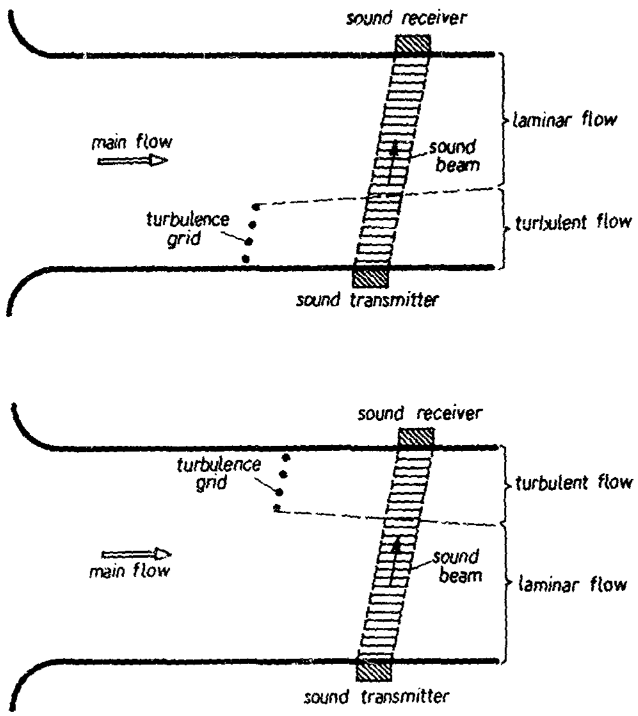

Fig.20: Sketch explaining the method used to check the influence of forward scattering on the measurements of the damping ΔI by turbulent scattering.

of the sound beam. If it was placed at the bottom of the tunnel, for instance (upper sketch of fig.20), only the lower part of the flow was made turbulent, if it was shifted towards the top of the test duct (as is shown in the lower sketch of fig.20), the upper third of the flow was turbulent only. The dimensions of the grid (M = 2.50 cm, D = 1.00 cm) and its distance from the sound beam axis (d = 5.0 cm) was chosen to obtain a value of $R_a \gtrsim 10$ at a sound frequency of 435 kcps. If at these conditions the forward scattering would have caused any effect, the damping ought to have been reduced systematically if the grid was shifted upwards. For, because of the same

deflection angle, scattered sound which is produced in the first part of the sound path surely reaches the diaphragm of the microphone by a smaller amount than scattered sound produced in its last part near the microphone. Such effect could not be observed. Thus, the results of the measurements presented in Section 4. in which $R_a \approx 10$ was never exceeded markably, had not to be corrected.

A further confirmation of this result follows directly from the measurements presented in the figs.13 to 15: If one considers measuring points which belong to any constant frequency of sound, one is sure that the value of R_a is equal for these points which were obtained by varying q only. For, $L_n \sim r_a \sim R_a$ is - with a good approximation - independent of the dynamic pressure q of the main flow. If one assumes (according to an estimate given in [1]) that at a given value of R_a or ν, respectively, all the scattered sound generated within a certain region before the microphone (the size of which depends on R_a only and increases with it) is received by the microphone, the length s on which the sound is scattered seems to be shortened by a value s_o depending on ν only. Hence, if forward scattering plays a role, the ΔI-points for different frequencies ν could not lie on one single curve because of the dependence of s_o on ν. But as the figures show they do lie well on one curve. Therefore, one can conclude again that forward scattering does not cause markable errors in ΔI.

Acknowledgements.

The author is most grateful to Professor Dr. W.Tollmien, Director of the Max-Planck-Institut für Strömungsforschung, and to Dr. E.-A.Müller and Dr. K.R.Matschat for numerous valuable discussions and suggestions which were very important for the advance of the present investigations. Moreover, he wishes to express his thanks to Dipl.-Phys. K.Kirde for his indefatigable help in the numerical evaluation of the

measuring curves obtained, and to Miss J.Krüger, Mr. H.Heinemann and Miss L. von Seebach for their assistance in preparing and typewriting this paper.

BIBLIOGRAPHY

[1] E.-A.Müller and K.R.Matschat: The scattering of sound by a single vortex and by turbulence. AFOSR TN 59-337, AD 213 658 (1959).

[2] D.I.Blokhintsev: Propagation of sound in an inhomogeneous moving medium. Doklady Akad. Nauk SSSR 45 (1944), 8, pp.343-346. (See also J.Acoust.Soc.Am. 18 (1946), pp.329-334.)

[3] M.J.Lighthill: On the energy scattered from the interaction of turbulence with sound or shock waves. Proc.Cambr.Phil.Soc. 49 (1953), pp.531-551.

[4] R.H.Kraichnan: The scattering of sound in a turbulent medium. J.Acoust.Soc.Am. 25 (1953), pp.1096-1104. Errata: J.Acoust.Soc.Am. 28 (1956), p.314.

[5] G.K.Batchelor: Wave scattering due to turbulence. Proc. 1st Symp. on Naval Hydrodynamics 1956, pp.409-430.

[6] V.A.Krasil'nikov and K.M.Ivanov-Shits: Some recent experiments on the propagation of sound in the atmosphere. Doklady Akad. Nauk SSSR 67 (1949), 4, pp.639-642.

[7] U.Ingard and F.M.Wiener: On the scattering of sound by atmospheric turbulence. J.Acoust.Soc.Am. 30 (1958), p.670.

[8] M.A.Kallistratova: Experimental investigations of the scattering of sound in the turbulent atmosphere. Doklady Akad. Nauk SSSR 125 (1959), 1, pp.69-72.

[9] D.C.Whitmarsh, E.Skudrzyk, R.J.Urick: Forward scattering of sound in the sea and its correlation with the temperature microstructure. J.Acoust.Soc.Am. 29 (1957), pp.1124-1143.

[10] W.Kuhl, G.R.Schodder, F.-K.Schröder: Condenser transmitters and microphones with solid dielectric for airborne ultrasonics. Acustica 4 (1954), pp.519-531.

[11] D.W.Schmidt: Verwendung von Ultraschallimpulsen zur genauen Messung von Strömungsgeschwindigkeiten. Diplomarbeit Göttingen 1956, Bericht Nr. 56/B/12 des Max-Planck-Instituts für Strömungsforschung.

[12] B.Chance a.o.: Waveforms. (Rad.Lab.Ser. 19). McGraw-Hill Book Co., Inc., New York 1949.

[13] J.O.Hinze: Turbulence. McGraw-Hill Book Co., Inc., New York 1959.

[14] A.Roshko: On the development of turbulent wakes from vortex streets. NACA Rep.No. 1191 (1954).

[15] G.K.Batchelor: The theory of homogeneous turbulence. Cambridge University Press, Cambridge 1953.

[16] S.F.Hoerner: Fluid-dynamic drag. Published by the author, New Jersey 1958.

[17] H.L.Dryden, G.B.Schubauer, W.C.Mock,Jr., H.K.Skramstad: Measurements of intensity and scale of wind-tunnel turbulence and their relation to the critical Reynolds number of spheres. NACA Rep.No. 581 (1937).

[18] H.Sato: Experimental study of the spectrum of isotropic turbulence I. J.Phys.Soc.Japan 6 (1951), pp.387-392.

[19] H.Tsuji and F.R.Hama: Experiment on the decay of turbulence behind two grids. J.Aero.Sci. 20 (1953), pp.848-849.

[20] H.L.Grant and I.C.T.Nisbet: The inhomogeneity of grid turbulence. J.Fluid Mech. 2 (1957), pp.263-272.

[21] J.Kestin and P.F.Maeder: Influence of turbulence on transfer of heat from cylinders. NACA TN 4018 (1957).

[22] R.R.Mills,Jr., A.L.Kistler, V.O'Brien, S.Corrsin: Turbulence and temperature fluctuations behind a heated grid. NACA TN 4288 (1958).

[23] B.G. van der Hegge Zijnen: Measurements of the intensity, integral scale and microscale of turbulence downstream of three grids in a stream of air. Appl.Sci.Res., Section A, 7 (1958), pp.149-174.

[24] A.A.Townsend: Momentum and energy diffusion in the turbulent wake of a cylinder. Proc.Roy.Soc. London, A, 197 (1949), pp.124-140.

[25] E.Frankenberger: Über den Austauschmechanismus der Bodenschicht und die Abhängigkeit des vertikalen Massenaustauschs vom Temperaturgefälle nach Untersuchungen an den 70 m hohen Funkmasten in Quickborn/Holstein. Ann.d.Meteorologie 1948, Beiheft I.

[26] E.Frankenberger: Über den Vertikalaustausch. Beitr.Phys. Atmos. 32 (1958), S.283-299.

[27] P.H.Parkin and W.E.Scholes: Air-to-ground sound propagation. J.Acoust.Soc.Am. 26 (1954), pp.1021-1023.

Max-Planck-Inst. AFOSR Contract:
f.Strömungsforsch. Rep.No.2 AD AF 61(514)-1143
Göttingen

Field: Mechanics

Monitoring Agency: Air Force Office of Scientific Research, AFOSR

EXPERIMENTAL INVESTIGATIONS ON THE SCATTERING OF SOUND BY TURBULENCE. Dieter W.Schmidt. July 1961. 60 pages,20 figs.

Wind tunnel investigations of the scattering of sound by turbulence were performed. Recent theoretical predictions are confirmed and partly extended by the measurements. In the range of the parameters which is of interest for practical use the most important results are the proportionality of the sound damping to the square of the sound frequency and to the square of the turbulent Mach number. A formula is derived from which the turbulent damping of directed sound (such as aircraft noise in the free atmosphere) can be calculated.

USAF, European Office, ARDC, Brussels, Belgium

Max-Planck-Inst. AFOSR Contract:
f.Strömungsforsch. Rep.No.2 AD AF 61(514)-1143
Göttingen

Field: Mechanics

Monitoring Agency: Air Force Office of Scientific Research, AFOSR

EXPERIMENTAL INVESTIGATIONS ON THE SCATTERING OF SOUND BY TURBULENCE. Dieter W.Schmidt. July 1961. 60 pages,20 figs.

Wind tunnel investigations of the scattering of sound by turbulence were performed. Recent theoretical predictions are confirmed and partly extended by the measurements. In the range of the parameters which is of interest for practical use the most important results are the proportionality of the sound damping to the square of the sound frequency and to the square of the turbulent Mach number. A formula is derived from which the turbulent damping of directed sound (such as aircraft noise in the free atmosphere) can be calculated.

USAF, European Office, ARDC, Brussels, Belgium

Max-Planck-Inst. f.Strömungsforsch. Göttingen

AFOSR Rep.No.2 AD

Contract: AF 61(514)-1143

Field: Mechanics

Monitoring Agency: Air Force Office of Scientific Research, AFOSR

EXPERIMENTAL INVESTIGATIONS ON THE SCATTERING OF SOUND BY TURBULENCE. Dieter W.Schmidt. July 1961. 60 pages,20 figs.

Wind tunnel investigations of the scattering of sound by turbulence were performed. Recent theoretical predictions are confirmed and partly extended by the measurements. In the range of the parameters which is of interest for practical use the most important results are the proportionality of the sound damping to the square of the sound frequency and to the square of the turbulent Mach number. A formula is derived from which the turbulent damping of directed sound (such as aircraft noise in the free atmosphere) can be calculated.

USAF, European Office, ARDC, Brussels, Belgium

Max-Planck-Inst. f.Strömungsforsch. Göttingen

AFOSR Rep.No.2 AD

Contract: AF 61(514)-1143

Field: Mechanics

Monitoring Agency: Air Force Office of Scientific Research, AFOSR

EXPERIMENTAL INVESTIGATIONS ON THE SCATTERING OF SOUND BY TURBULENCE. Dieter W.Schmidt. July 1961. 60 pages,20 figs.

Wind tunnel investigations of the scattering of sound by turbulence were performed. Recent theoretical predictions are confirmed and partly extended by the measurements. In the range of the parameters which is of interest for practical use the most important results are the proportionality of the sound damping to the square of the sound frequency and to the square of the turbulent Mach number. A formula is derived from which the turbulent damping of directed sound (such as aircraft noise in the free atmosphere) can be calculated.

USAF, European Office, ARDC, Brussels, Belgium

UNCLASSIFIED

UNCLASSIFIED